Proceeding for International Conference

on

Emerging Trends in

Engineering and Technology

Pune

1st November' 15

Institute for Engineering Research and Publication

Editorial:

We cordially invite you to attend the International Conference on Emerging Trends in Engineering and Technology (ICET-15), which will be held in Lakme Executive The Business Hotel, Pune on November 1, 2015. The main objective of ICET-15 is to provide a platform for researchers, engineers, academicians as well as industrial professionals from all over the world to present their research results and development activities in Electrical, Electronics, Mechanical, Civil and Computer Science Engineering. This conference provides opportunities for the delegates to exchange new ideas and experience face to face, to establish business or research relations and to find global partners for future collaboration.

These proceedings collect the up-to-date, comprehensive and worldwide state-of-art knowledge on software engineering, computational sciences and computational science application. All accepted papers were subjected to strict peer-reviewing by 2-4 expert referees. The papers have been selected for these proceedings because of their quality and the relevance to the conference. We hope these proceedings will not only provide the readers a broad overview of the latest research results on Electrical, Electronics and Computer Science Engineering but also provide the readers a valuable summary and reference in these fields.

The conference is supported by many universities and research institutes. Many professors plaid an important role in the successful holding of the conference, so we would like to take this opportunity to express our sincere gratitude and highest respects to them. They have worked very hard in reviewing papers and making valuable suggestions for the authors to improve their work. We also would like to express our gratitude to the external reviewers, for providing extra help in the review process, and to the authors for contributing their research result to the conference.

Since October 2015, the Organizing Committees have received more than 120 manuscript papers, and the papers cover all the aspects in Electrical, Electronics, Mechanical, Civil and Computer Science Engineering. Finally, after review, about 10 papers were included to the proceedings of ICET- 2015.

We would like to extend our appreciation to all participants in the conference for their great contribution to the success of International Conference 2015. We would like to thank the keynote and individual speakers and all participating authors for their hard work and time. We also sincerely appreciate the work by the technical program committee and all reviewers, whose contributions make this conference possible. We would like to extend our thanks to all the referees for their constructive comments on all papers; especially, we would like to thank to organizing committee for their hard work.
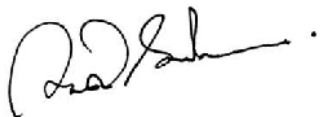
Editor-In-Chief
Dr. Nalini Chidambaram
Professor
Bharth University

Acknowledgement

IFERP is hosting the International Conference on Emerging Trends in Engineering and Technology this year in month of November. Technical advantage is the backbone of development and nanoelectronics has become the platform behind all the sustainable growth International Conference on Emerging Trends in Engineering and Technology will provide a forum for students, professional engineers, academician, scientist engaged in research and development to convene and present their latest scholarly work and application in the industry. The primary goal of the conference is to promote research and developmental activities in Electronics, Electrical, Mechanical, Civil, Computer Science and Information Technology and to promote scientific information interchange between researchers, developers, engineers, students, and practitioners working in and around the world. The aim of the Conference is to provide a platform to the researchers and practitioners from both academia as well as industry to meet the share cutting-edge development in the field.

I express my hearty gratitude to all my Colleagues, staffs, Professors, reviewers and members of organizing committee for their hearty and dedicated support to make this conference successful. I am also thankful to all our delegates for their pain staking effort to travel such a long distance to attain this conference.

Er. R. B. Satpathy
Secretary
Institute for Engineering Research and Publication (IFERP)

CONTENTS

ORGANIZATION COMMITTEE

MANAGING DIRECTOR
Dr. P. C. Srikanth
Head of the Department,
Department of ECE,
Malnad College of Engineering

PRESIDENT:
Dr. P A Vijaya
Professor, Department of ECE,
BNM Institute of Technology

ORGANIZING SECRETARY
Asst. Prof. Bonia Mohan,
Department of CSE,
Dayananda sagar College of Engineering,
Bangalore,

PUBLICATIONS COMMITTEE
Dr. Shankar Narayanan
Dr.S. Sangeetha

PROGRAM CHAIR
Dr. Nalini Chidambaram
Professor
Bharth University

SafePass – A Secure, Easy to Integrate Login API for Websites using Picture and Map Password

[1]Aditya Medhe,[2]Sachin Yadav,[3]Shivprasad Hande
[1][2][3]Maharashtra Institute of Technology, Pune
[1]adityamedhe3@gmail.com,[2]sachydv@gmail.com,[3]prasad_hande20@yahoo.in

Abstract- **SafePass is a web service which provides an API (Application Programming Interface) for client websites to inculcate a secure, picture based and maps based password authentication system. Using SafePass, using just one line of code, websites can integrate picture password authentication into them which is then completely handled by the SafePass web service. The user using a SafePass client website is presented a SafePass login screen when he logs in. Then, he enters his picture password or a map route password which is matched by the algorithm with the stored pattern. If the pattern is correct, then SafePass provides all the details of the user to the web site and authenticates him. The picture password and the matching algorithm provide a high degree of randomness and hence are very strong to be cracked.**

Key words- **login, picture password, map password, API, authentication**

I. INTRODUCTION

One of the key areas in security research and practice is authentication, the process of determining whether a user should be allowed access to a given system or resource. Traditionally, alphanumeric passwords have been used for authentication. Today other methods, including biometrics and smart cards, are possible alternatives. However, passwords are likely to remain widely used for some time because of drawbacks of reliability, security, or cost of other technologies. In particular, smart cards also need PINs and passwords, while biometrics raises privacy concerns.

The security and usability problems associated with alphanumeric passwords are collectively called as „„the password problem.‟‟ The password problem arises because passwords are expected to comply with two conflicting requirements, namely:

A. *Passwords should be easy to remember*, and the user authentication process should be executable quickly and easily by humans.

B. *Passwords should be secure*, i.e. they should look random and should be hard to guess; they should be changed frequently, and should be different on different accounts of the same user; they should not be written down or stored in plain text. Meeting both of these requirements is almost impossible for users. The problem is well known in the security community. Studies going back over 25 have shown that, as a result, human users tend to choose and handle alphanumeric passwords very insecurely.

II. BLONDER‟S ALGORITHM

Greg E. Blonder created this method in 1996. In this method, a pre-determined image is presented to the user on a visual
display and then the user is required to tap regions by pointing to one or more predefined locations that are present on the image (in a predetermined order) as a way of proving his or her authorization to access the resource. According to Blonder this method is secure since it has a million of different regions to pick from.

Demerits: The drawback to this algorithm was that the amount of predefined click regions was small so the password had to be quite long in order for it to be secure. Another drawback is, the use of pre-defined click objects or regions meant that simple, artificial images, for example cartoon-like images, were supposed to be used in place of complex real world scenes.

III. PASSPOINT ALGORITHM

The major shortcoming of Blonder‟s Algorithm is that it has a very small password space. This is overcome in our algorithm.
The „„password space‟‟ is the set of all passwords that are possible for a given password scheme and for a given setting of parameters. For example, for alphanumeric passwords of length eight over a 64-character alphabet, the number of possible passwords is $64^8=2.8*10^{14}$. In our graphical password scheme, as we tested it in our empirical study, with image size 451*331 and grid square size 20*20 (all

measured in pixels)there are about 451*331/20*20 = 373 grid squares; hence, for passwords consisting of five click points, the password space has size $373^5 = 7.2*10^{12}$. . With the same settings, but with six click points, the password space has size $373^6 = 2.69*10^{15}$. If in our graphical password scheme the image size is 1024*752 (roughly the full screen), with grid square size still 20*20 (all measured in pixels), and with passwords consisting of five clicks, the password space will have size $2.6*10^{16}$.

IV.   PICTURE PASSWORD

A picture password is basically an innovative type of password which involves drawing gestures such as lines and circles on a user-chosen image. Since the image is of familiarity to the user, the gestures are very hard to forget. At the same time, they offer a high degree of randomness and hence cannot be cracked easily by a third party.

The sequence as well as   the direction of the entered gestures are also taken into   consideration during matching, further increasing the strength. During login, the user has to draw (approximately) the same gestures as he did during the set up to authenticate himself.

To improve upon the shortcomings of the Blonder Algorithm, in 2005, PassPoint was created. Passpoint was able to overcome the
drawbacks of Blonder‟s algorithm to some extent. In   this case the image could be any natural picture or painting   as well as any complex image   so as to have several possible click points. Apart from this, a major difference is that the image is not secret and has no other role other than that of assisting the user to remember   the click point. More importantly, it is not as rigid as the   Blonder‟s algorithm which requires the setting of artificial predefined click regions with well-marked boundaries.

The authentication process involves the user selecting several points on picture in a particular order. When logging in, the user is supposed to click close to the selected click points, within some (adjustable) tolerance distance, for instance within 0.25 cm from the actual click point.

Figure 1. *Example of a picture password*

V.   MAP PASSWORD

A map password is similar to a picture password except it involves drawing a route on a map to authenticate the user. Since the map can be zoomed in as much as the user wishes and no. of locations are practically unlimited, this method offers a high degree of randomness and security.

A major drawback to using passwords is that very good passwords are difficult to remember without any errors during the authentication and the ones that are easy to remember are too short and simple to be secure. All in all studies on human memory indicate that it is quite straightforward to remember landmarks on a well-known journey.

This suggests that we can use a map as an alternative. For example, if a user embarked on a memorable journey some time in his life, he can very well recreate the route of the journey and can enter it on the map without any difficulty. This fact can be leveraged to create a map password. Coupling this concept with the readily available and complete maps provided by public APIs, the task of implementing this type of password becomes easy as well as a fool proof and secure way of authentication.
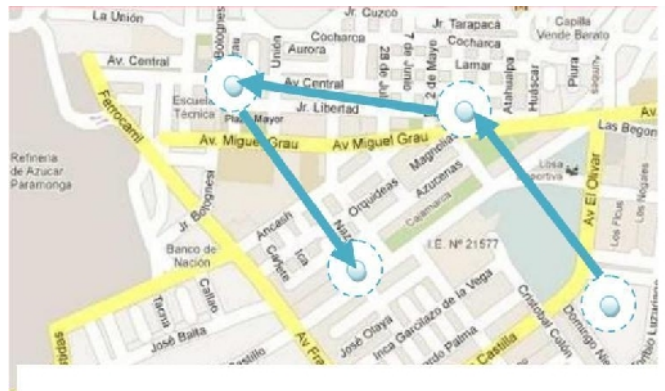
Figure 2. Example of a Map Password

VI.   AUTHENTICATION USING API

This system is being implemented not as a standalone system, rather as an API (Application Programming Interface) for the internet. Developers who wish to integrate these types of password authentication on their websites can do so with a few lines of program code. The protocol that we are using for the data exchange is a simplified version of the OAuth 2.0 protocol which is used by all major social networks for providing login facility.

This protocol relies on different types of tokens to securely exchange data between the applications. The developer of

the web site has to first register as an API Client, which will enable him to access the API using a secret key. Users of the system who log in using this method will be given total control over their data and who can access it.
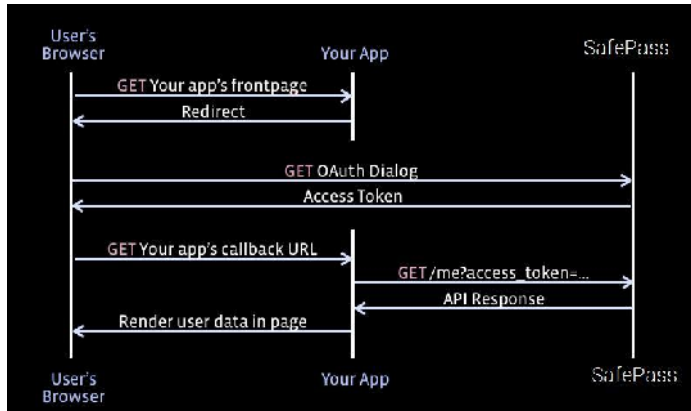
Figure 3. *Simplified version of OAuth protocol to be used*

REFERENCES

[1] Arash Habibi Lashkari, Abdullah Gani, Leila Ghasemi

Sabet and Samaneh Farmand, "*A new algorithm on Graphical User Authentication (GUA) based on multi-line grids*".

[2] S.Rajarajan, M. Prabhu, S. Palanivel, M.P.Karthikeyan,

"*Gramap: Three Stage Graphical Password Authentication Scheme*", Journal of Theoretical and Applied Information
Technology, March 2014.

[3] Julie Thorpe, Brent MacRae, Amirali Salehi-Abari,

"*Usability and Security Evaluation of GeoPass: a Geographic Location-Password Scheme*", Symposium on Usable Privacy and Security (SOUPS) 2013, July 24–26, 2013, Newcastle, UK

[4] Susan Wiedenbeck, Jim Waters, Jean-Camille Birget, Alex

Brodskiy, Nasir Memon, "*PassPoints: Design and longitudinal evaluation of a graphical password system*",
Int. J. Human-Computer Studies (2005).

● ● ●

An Acoustic Dialogued Based Interface Using Dynamic Time Wrapping Technique

[1]Ms.Anuradha J.Bhatt,[2]Dr.M.V.Sarode

Controller of Examination, GIPT, Mumbai

Ast. Professor, J.C.O.E.T, Yavatmal

Abstract- **An acoustic dialogued based system provides interface between human and computer as well as execute specific action based on this command. Owing to the developments in human computer interface, human and computer has seized communication gap. Basically this experiment is carried out for seven commands using low cost microphone. Considering applications of this interface in medical field, the experiment is aimed at identifying speech by minimizing speckles noise effect with optimum solution for execution of commands. Beside traditional interfaces support sequential and unambiguous input from devices such as keyboard and conventional pointing devices, speech driven dialogue-based interfaces relax these constraints and typically incorporate a broader range of input devices for example spoken language, pen, touch screen, displays, keypads, pointing devices, and tactile sensors. This interface consists of design of a dialogue-enabled HCI system for collaborative decision making, command, and control.**

Key words- **human computer interface (HCI), acoustic analysis, speech, audio**

I. INTRODUCTION AND BACKGROUND

Speech is a natural mode of communication for people. We learn all the relevant skills during early childhood, without instruction, and continue to rely on speech communication throughout our lives. It comes so naturally to us that there is no realization of its complexity. Communication among the human being is dominated by spoken language, therefore it is natural for people to expect speech interfaces with computer, which can speak and recognize speech in native language [2]. The human vocal tract and articulators are biological organs with nonlinear properties, whose operation are not just under conscious control but also affected by factors ranging from gender to upbringing to emotional state. As a result, vocalizations can vary widely in terms of their accent, pronunciation, articulation, roughness, nasality, pitch, volume, and speed; moreover, during transmission, our irregular speech patterns can be further distorted by background noise and echoes, as well as electrical characteristics (if telephones or other electronic equipment are used). Speech is produced by modulating a relatively small number of parameters of a dynamical system [3], and this implies that its true underlying structure is much lower-dimensional than is immediately apparent in a window that contains hundreds of coefficients. We believe, therefore, that other type. All these sources of variability make speech recognition, evenmore than speech generation, a very complex problem. The following figure shows design flow for speech recognition technique consisting of five steps as:
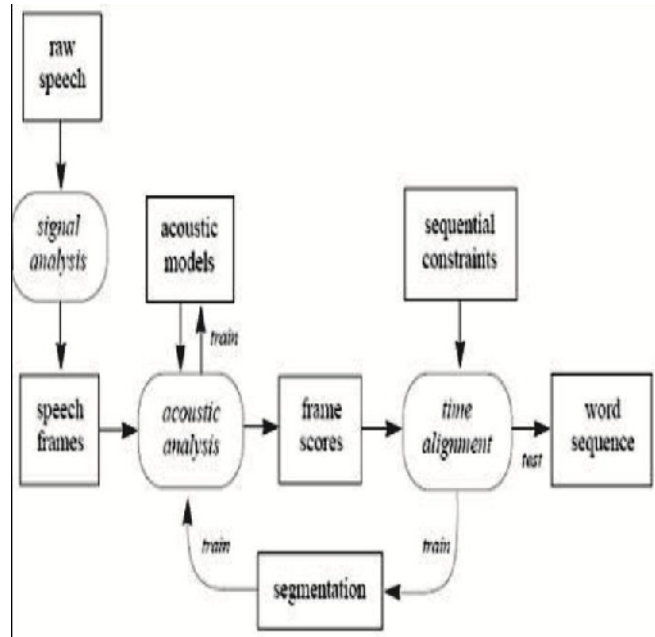
Figure 1: Design flow for speech recognition technique

1. speech- Speech is typically sampled at a high frequency, e.g., 16 KHz over a microphone or 8 KHz over a telephone. This yields a sequence of amplitude values over time.
2. Signal analysis- Raw speech should be initially transformed and compressed, in order to simplify subsequent processing Among the most popular: Fourier analysis (FFT), Perceptual Linear Prediction (PLP), Linear Predictive Coding (LPC) .

3. Spectral analysis calculates the inverse Fourier transform of the logarithm of the power spectrum of the signal. In this step for removing speckle noise a kalman filter is used, the Kalman filter is a tool that can estimate the variables of a wide range of processes. In mathematical terms a Kalman filter estimates the states of a linear system.
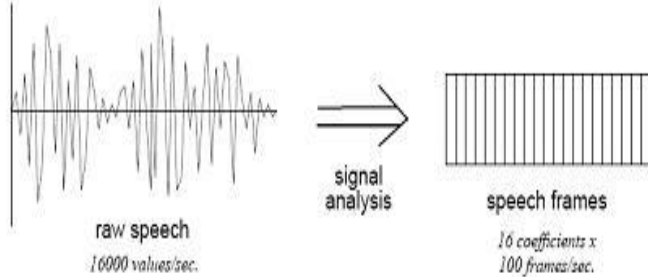

Figure 2: Signal Analysis of raw speech into speech frames

4. Speech frames- The result of signal analysis is a sequence of speech frames, typically at 10 m sec intervals, with about 16 coefficients per frame as represented in figure 2
5. Acoustic models- There are many kinds of acoustic models, varying in their representation, granularity, context dependence, and other properties.
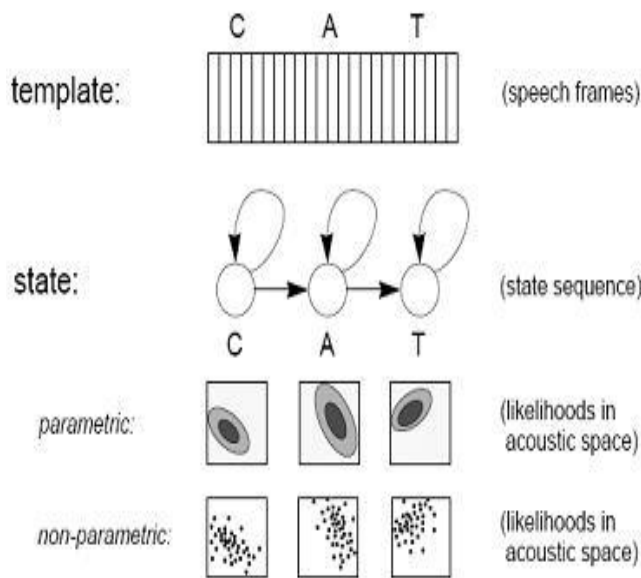

Figure 3: Acoustic models showing template and state representations for the word "cat".

Above figure 3 shows two popular representations for acoustic models. The simplest is a template, which is just a stored sample of the unit of speech to be modeled, for example a recording of a word. An unknown word can be recognized by simply comparing it against all known templates, and finding the closest match. A more flexible representation, used in this interface, is based on trained acoustic models, or states. In this approach, every word is modeled by a sequence of trainable states, and each state indicates the sounds that are likely to be heard in that segment of the word, using a probability distribution over the acoustic space. Probability distributions can be modeled parametrically, by assuming that they have a simple shape (e.g., a Gaussian distribution) and then trying to find the parameters that describe it; or non-parametrically, by representing the distribution directly (e.g., with a histogram over a quantization of the acoustic space, or, as we shall see, with a neural network). The remaining paper is organized to discuss methodology of acoustic dialogued based interface in section II, experimental results in section III, followed by conclusions in section IV.

II. PROPOSED METHODOLOGY

Dynamic systems (this is, systems which vary with time) are often represented in a state-space model. State-space is a mathematical representation of a physical system as a set of inputs, outputs and state variables related linearly. The Kalman filter addresses the general problem of trying to estimate the state of a discrete-time controlled process that is governed by the models below
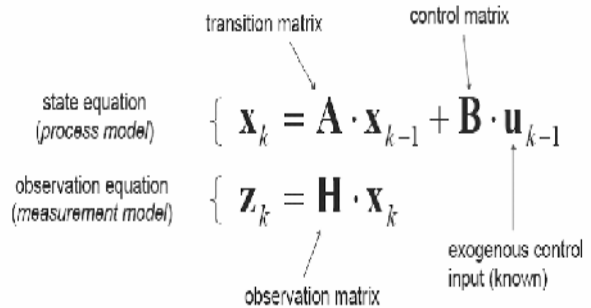
In addition to this, a random, Gaussian, white noise source w_k and v_k are added to the state and observation equations respectively. The process noise w has a covariance matrix Q and the measurement noise v has a covariance matrix R, which characterizes the uncertainties in the states and correlations within it. At each time step, the algorithm propagates both a state estimate x_k and an estimate for the error covariance P_k, also known as a priori estimates. The latter provides an indication of the uncertainty associated with the current state estimate. These are the predictor equations. The measurement update equations (corrector equations) provide a feedback by incorporating a new measurement value into the a priori estimate to get an improved a posteriori estimate.

The Kalman Gain is derived from minimizing the a posteriori error covariance. The Kalman Gain is the measurement error covariance R approaches zero, the actual measurement z is "trusted" more and more, while the predicted measurement H_x is trusted less and less. On the other hand, as the a priori estimate error covariance P approaches zero the actual measurement is trusted less and

less, while the predicted measurement is trusted more and more.

Dynamic time warping (DTW) is a time series alignment algorithm developed originally for speech recognition. It aims at aligning two sequences of feature vectors by warping the time axis iteratively until an optimal match (according to a suitable metrics) between the two sequences is found. Consider two sequences of feature vectors:

$$A = a_1, a_2, ………..a_i…………,a_n$$

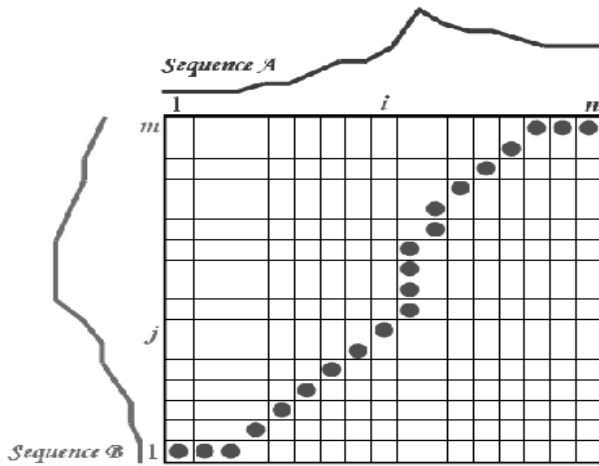$$B = b_1, b_2,…… …b_j…………,b_m$$

Figure 4 : Graph showing working of Dynamic Time wrapping algorithm

Inside each cell a distance measure can be placed, comparing the corresponding elements of the two sequences. To find the best match or alignment between these two sequences one need to find a path through the grid which minimizes the total distance between them. The procedure for computing this overall distance involves finding all possible routes through the grid and for each one computes the overall distance. The overall distance is the minimum of the sum of the distances between the individual elements on the path divided by the sum of the weighting function. The weighting function is used to normalize for the path length. It is apparent that for any considerably long sequences the number of possible paths through the grid will be very large. The major optimizations or constraints of the DTW algorithm arise from the observations on the nature of acceptable paths through the grid:

1. Monotonic condition: the path will not turn back on itself, both the i and j indexes either stay the same or increase, they never decrease.
2. Continuity condition: the path advances one step at a time. Both i and j can only increase by at most 1 on each step along the path.
3. Boundary condition: the path starts at the bottom left and ends at the top right.

4. Wrapping window condition: a good path is unlikely to wander very far from the diagonal. The distance that the path is allowed to wander is the window width.
5. Slope constraint condition: The path should not be too steep or too shallow. This prevents short sequences matching too long ones. The condition is expressed as a ratio p/q where p is the number of steps allowed in the same (horizontal or vertical) direction. After p steps in the same direction is not allowed to step further in the same direction before stepping at least q time in the diagonal direction.

III. EXPERIMENTAL RESULT

A dialogued based interface consists of seven commands mentioned below. Based on this command the system give response in terms of specific action

Input Command	Response Action
Select 1	First Image is selected
Select 2	Second image is selected
Select 3	Third image is selected
Move To Left	Desired image is moved to Left
Move To Right	Desired image is moved to Right
Move To Bottom	Desired image is moved to Bottom
Move To Top	Desired image is moved to Top

Table 1: User Interface commands with respective response.

Initially live speech is capture by using microphone or mike and then it is converted into digitized frames, which is further divided to be processed by kalman filter and dynamic time wrapping algorithm is applied on this signal. After command "Move To Left" is said, the selected image is moved to left as demonstrated in figure 5. If we say "Move to Right" selected image is moved to right as shown in figure 6, while for "Move To Bottom" the selected image is moved to Bottom. Similarly for "Move To Top" selected image is moved to Top. Thus various command are given to the system for different movements like move left, right, bottom, top depending on utility. Using these commands the selected image moves left and right, bottom and top respectively.
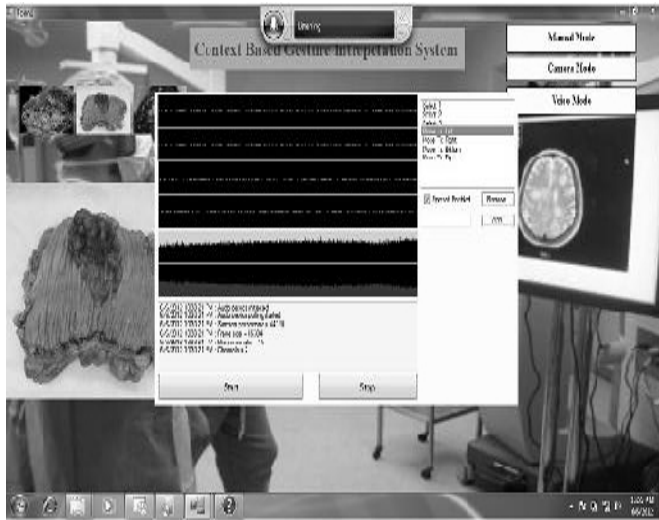
Figure 5: User Interface demonstrating speech recognition for said command "Move To Left".
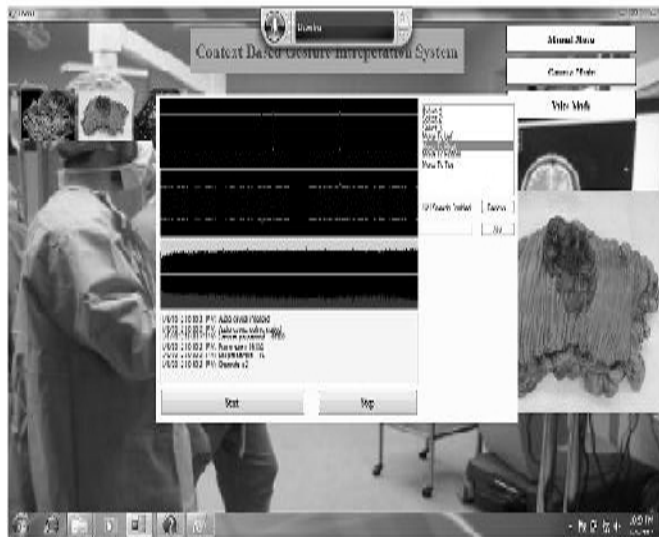

Figure 6: User Interface demonstrating speech recognition for said command "Move To Right".

The dialogue based speech recognition interface is speaker dependent and needs to be trained for individual users. Hence, it would be useful to experiment with other speech recognition products. Accuracy of this interface is 96% in a clean environment. However, environment where there is disturbance can lead to a 20%-30% drop in speech recognition accuracy.

CONCLUSION

This paper represents an experiment for ongoing work in building technologies to improve natural human-machine interaction. A proposed interface is having ability to interpret user's speech and hand gesture in real time to manipulate medical image visualization environment. The main goal of this experiment is to create a system which can recognize specific dialogue and use them to convey information for device control. An acoustic dialogue is used for expressing ones ideas and information associated in a conversation degree, discourse structure, spatial and temporal structure. Recognition of speech has been implanted successfully by means of dynamic time wrapping algorithm. Quality of system depends on how it is represented and used by user. Therefore, enormous amount of attention has been paid to improve the accuracy of system.

Future work includes analyzing and responding to more vocabulary for speech module. The results can further be improved by training the system for more dialogued, which are required for all these basic movements of the system.

REFERENCE

[1] Sarikaya R., Gao Y., Erdogan H., and Picheny M., "*Turn-Based Language Modeling for Spoken Dialog Systems,*" in Proceedings of IEEE International Conference on Acoustics, Speech, and Signal Processing, vol. 1, pp. I 81-I-784, 2002.

[2] Olsen, J., Cao, Y., Ding, G. & Yang, X. "*A decoder for large vocabulary continuous short message dictation on embedded devices*", IEEE International Conference on Acoustics, Speech and Signal Processing , pp. 4337–4340.2008.

[3] Geoffrey Hinton, Li Deng, Dong Yu, George Dahl, Abdel-rahman Mohamed, Navdeep Jaitly, Andrew Senior,Vincent Vanhoucke, Patrick Nguyen, Tara Sainath, andBrian Kingsbury, "Deep Neural Networks for Acoustic Modeling in Speech Recognition" SIGNAL PROCESSING MAGAZINE IEEE 2012.

[4]A Stolcke, "Making the most from multiple microphones in meeting recognition," in Proc IEEE ICASSP, 2011.

[5] Chin-Tuan Tan and Brian C. J. Moore, Perception of nonlinear distortion by hearing-impaired people, International Journal of Ideology 2008, Vol. 47, No. 5 , Pages 246-256.

[6]M. D. McNeese and M. A. Vidulich, "*Cognitive Systems Engineering in Military Aviation Environments: Avoiding Cogminutia Fragmentosa",* Wright-Patterson AFB, OH: Human Systems Information Analysis Center, 2002.

[7]Anuradha Bhatt, S.A.Chabria, Mukta Bhatt, " *A context based human interpretation system"* Proceedings published in International Journal of Computer Applications 2011

●   ●   ●

A Recent Study on Indian Number Plate Recognition Using Optical Character Recognition

[1]Ashwini Mhetre,[2]Dhanashri Deosarkar,[3]Priya Devkate,[4]Prof. S.S.Pattanaik

[1][2][3][4]Department of Computer Engineering,JSPM's Rajarshi Shahu College Engineering, Pune, India

Abstract- **With the development of vehicles and the increasing number of cars in modern society, people pay more and more attention to the vehicle license plate recognition system. Vehicle license plate recognition is divided into three parts: license positioning, character segmentation and character recognition. One of the method is Automatic Number Plate Recognition (ANPR) is a real time embedded system which automatically recognizes the license number of vehicles. In this paper, with the help of this technique the task of recognizing number plate for Indian conditions is considered, where number plate standards are rarely followed. The propose architecture uses integration of algorithms like: 'Feature-based number plate Localization' for locating the number plate, 'Image Scissoring' for character segmentation and statistical feature extraction for character recognition; which are specifically designed for Indian number plates. As per the Indian number plate patterns by using this method and by implementing these algorithms in Java we can achieve to recognize one or two line number plate almost perfectly. And due to use of higher level language in this paper we can achieve more flexibility and security in implementing those algorithms.**

Key words- **Automatic license plate recognition (ALPR), automatic number plate recognition (ANPR), car plate recognition (CPR), and optical character recognition (OCR) for cars.**

I. INTRODUCTION

The existing methods and systems for optical character recognition provide high reliability of the recognition of texts with high and medium print quality. It contains very small type of errors which cannot be recognised by human being. However such systems are not always able to cope with the task of characters recognition in industrial systems, for example, while recognising serial numbers in products, packing etc. Automatic number plate recognition is a mass surveillance method that uses optical character recognition on images to read vehicle registration plates. They can use existing closed-circuit television or road-rule enforcement cameras, or ones specifically designed for the task. They are used by various police forces and as a method of electronic toll collection on pay and cataloguing the movements of traffic or individuals. ANPR can be used to store the images captured by the cameras as well as the text from the license plate, with some configurable to store a photograph of the driver. Systems commonly use infrared lighting to allow the camera to take the picture at any time of the day. ANPR technology tends to be region-specific, owing to plate variation from place to place. By considering these techniques and technology we have

decided to purpose a system which can be useful for visitor to recognize buses by their name board.

II. PREVIOUSLY WORK DONE

In paper [4] which is on An Image Segmentation Algorithm in Image Processing Based on Threshold Segmentation it is said that Image segmentation is a key technology in image processing, and threshold segmentation is one of the methods used frequently. Aimed at that only one threshold or several thresholds are set in traditional threshold-based segmentation algorithm, it is difficult to extract the complex information in an image; a new segmentation algorithm that each pixel in the image has its own threshold is proposed. In this algorithm, the threshold of a pixel in an image is estimated by calculating the mean of the grayscale values of its neighbor pixels, and the square variance of the grayscale values of the neighbor pixels are also calculated as an additional judge condition, so that the result of the proposed algorithm is the edge of the image. In fact the proposed algorithm is equal to an edge detector in image processing. Experimental results demonstrate that the proposed algorithm could produce precise image edge, while it is reasonable to estimate the threshold of a pixel through the statistical information of its neighbor pixels. By

studying this paper we get the concept of Segmentation Algorithm

Also in [5] the maximum entropy-based image segmentation approach is proposed to segment a gray-scale face image. The approach performs with the Maximum Entropy Thresholding value (MET) of 2D image. A target of experiment is reported face image segmentation that uses still face image from BioID database. The results of this method are clearly demonstrating the segmentation that performs better than other work on the same original image. Furthermore, the value of MET method gets threshold equal 141 that are both similar to the threshold segmentation with Centre of mass method (threshold = 139) and Iterative method (threshold = 140), but different from Otsu's method. It indicates a small sufficient step that can be used for face segmentation, detection, and extraction which are the next steps of the entire face recognition system. From this we get the concept of Segmentation Algorithm maximum Entropy.

III. SYSTEM ARCHITECTURE AND ALGORITHM USED

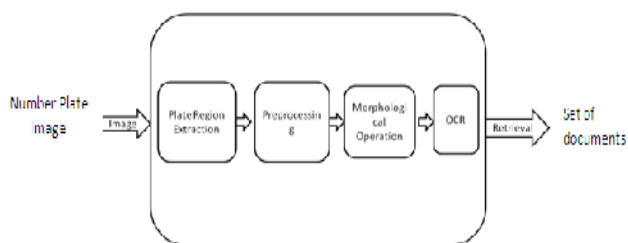Fig.1. shows the architecture diagram of the proposed system.

Fig.1. System Architecture

The proposed system accepts number plate image as input and a set of documents is retrieved from the system in form of output. The captured image goes through some intermediate process to get efficient output. The main idea of the proposed system is to extract a license plate number from given image. This process of automatic license plate recognition is composed of four stages. The stages are as follows:

1] Image Acquisition
2] License Plate Region Extraction
3] License Plate Segmentation
4] Optical Character Recognition (OCR)

Fig.2. shows the four stages of an Automated License Plate Recognition (ALPR) system.

Fig.2. Four Stages of ALPR System

1) Image Acquisition

In first stage, the license plate image is acquired using a camera. The parameters of the camera, such as the type of camera, camera resolution, orientation, and light, have to be considered.

2) License Plate Region Extraction

The second stage is to extract the license plate from the image based on some features. In the proposed system boundary based extraction is performed. The Boundary-based extraction technique uses Hough transform (HT)[9]. It detects straight lines in the image to locate the license plate. The Hough transform has the advantage of detecting straight lines with up to 30° inclination.

3) License Plate Segmentation

In this stage, the license plate is segmented and the characters are extracted by projecting their color information, labeling them, or matching their positions with templates. In this stage, binarization is performed. Binarization is usually performed in the preprocessing stage of different document image processing related applications such as optical character recognition (OCR) and document image retrieval. It converts a gray-scale document image into a binary document image and accordingly facilitates the ensuing tasks such as document skew estimation and document layout analysis.

4) Optical Character Recognition (OCR)

In this stage, the extracted characters are recognized and the output is the license plate number. Character recognition in ALPR systems may have some difficulties. Due to the camera zoom factor, the extracted characters do

not have the same size and the same thickness. Resizing the characters into one size before recognition helps overcome this problem.

CONCLUSION

Automatic License Plate Recognition (ALPR) System will process on images of number plate of cars and find out the details of car and owner. It will help police traffics to understand the detail of owner and car details and solve the problem of carry document This system consists of modules i.e. plate extraction, processing, morphological operations and OCR for character recognition. We have used edge and color detection algorithm for extraction, maximum entropy for binaries, morphological operation for noise removal and OCR for character recognition.

REFERENCES

[1] G. Liu, Z. Ma, Z. Du, and C. Wen, "The calculation method of road travel time based on license plate recognition technology," in Proc. Adv.Inform. Tech. Educ. Commun. Comput. Inform. Sci., 2011.

[2] Y.-C. Chiou, L. W. Lan, C.-M. Tseng, and C.-C. Fan, "Optimal locations of license plate recognition to enhance the origin-destination matrix estimation," in Proc. Eastern Asia Soc. Transp. Stu., 2011.

[3] S. Kranthi, K. Pranathi, and A. Srisaila, "Automatic number plate recognition," Int. J. Adv. Tech., 2011.

[4] C.-N. E. Anagnostopoulos, I. E. Anagnostopoulos, I. D. Psoroulas, V. Loumos, and E. Kayafas, "License plate recognition from still images and video sequences: A survey," IEEE Trans. Intell. Transp. Syst., Sep. 2008.

[5] C. Nelson Kennedy Babu and K. Nallaperumal, "An efficient geometric feature based license plate localization and recognition," Int. J. Imaging Sci. Eng., 2008.

[6] F. Faradji, A. H. Rezaie, and M. Ziaratban, "A morphological-based license plate location," in Proc. IEEE Int. Conf. Image Process., vol. Sep.–Oct. 2007

[7] D. Zheng, Y. Zhao, and J. Wang, "An efficient method of license plate location," Pattern Recognit. Lett., 2005.

[8] K. Kanayama, Y. Fujikawa, K. Fujimoto, and M. Horino, "Development of vehicle-license number recognition system using real-time image processing and its application to travel-time measurement," in Proc. IEEE Veh. Tech. Conf., May 1991.

[9] V. Kamat and S. Ganesan, "An efficient implementation of the Hough transform for detecting vehicle license plates using DSPs," Real-Time Tech. Applicat. Symp., 1995

● ● ●

Dynamic Simulation of Oil-fired Boiler

[1]A.B.Dhekale, [2]N.V.Borse, [3]R.S.Jha, [4]Sahir Mulla

[1] MIT College of Engineering, Pune, India ,[2] Vishwakarma Institute of Technology, Pune, India, [3] Thermax ,Pune, India, [4] Thermax, Pune, India

[1]ashwini.dhekale@gmail.com,[2] nvsborse@gmail.com, [3] jhars@thermaxIndia.com, [4]mullasahir@gmail.com

Abstract- **The three flue pass fire-tube boiler has been analyzed. A dynamic model has been developed for analysis of boiler performance. In the model, two parts of the boiler (Gas and water/steam) are considered. Gas side mainly consist of modeling of furnace, Internal Reversible Chamber (IRC), first convective pass and second convective pass. All of these models give detailed information about heat transfer from flue gas to water and also models provide temperature distribution along axial direction. Water/Steam side model analyses phase transformation phenomenon effectively. Module developed for capturing shrink and swell phenomenon due to bubble formation and collapse gives better results. Newton Raphson method has been used to calculate correct pressure value. Model developed can capture the dynamics of boiler level and boiler pressure. Also analysis of PID controller has been done with the help of which pressure change due to load change can be controlled. All the models developed have been integrated and simulated with the help of VBA/Excel.**

Suitability of the model has been checked against experimental results of boiler of 1 Ton capacity. Simulation of boiler gives better control of pressure and level at steady as well as dynamic conditions.

Key words- **Fire-tube boiler, Heat transfer, Modeling, Simulation,**

I. INTRODUCTION

The fire tube boiler consists of outer shell containing bundle of tubes inside. Hot flue gases flows inside the tubes and steam generation takes place outside the tubes. Fire tube boilers are generally classified on the basis of no. of times the flue gases pass along boiler length.

The fuel combustion takes place in a furnace and hot flue gases flows from the furnace to chimney through bundle of tubes.

Rigorous work on applications of boilers has been carried out since long. Some papers have been published regarding use of boilers for power and process[1].

Dynamics of boiler has great impact on performance of boiler, hence modeling and simulation of transient operations of systems in the boiler are becoming more important [2].

Several mathematical models for water tube boilers have been published [3]. In this work, the modeling of heat transfer from flue gas to water in a three flue pass fire-tube boiler is considered. The behavior of metal temperature together with shrink and swell phenomenon dominates the dynamics of boiler.

II. MATHEMATICAL MODELING

Any physical phenomenon that takes place in nature can be described in the form of mathematics. For any complex or simple physical system, mathematical model can be developed. Modeling enables to understand the behavior of system properly.

a) Gas side modeling

In furnaces, where fuel combustion takes place, temperature is above about 8000C. At these high temperatures, radiation is the dominant mode of heat transfer and it is important to estimate rates of radiative heat exchange in these furnaces. for lower temperatures , combined effect of convective and radiative heat transfer must be taken into account.

Plug flow furnace model has been selected after studying Stirred reactor, Plug flow and Multizone furnace models[4].

Among three furnace models, plug flow model gives distribution of heat flux within the furnace and also it is useful when furnace is long compared with its mean hydraulic radius. In this model, differential equations have been generated to solve for the axial temperature distribution in the furnace with the help of finite difference methods.

In 1986, Tucker observed that in systems with large temperature gradients, subdivision of the furnace into zones may be necessary and the variations of emissivity and/or

absorptivity will be required over a range of beam lengths and temperatures.[4]

b) Calculations for flue gas outlet temperature

In this work also, flue gas volume flowing along length of furnace has been divided into 50 no. of elements. heat balance equations have been applied To each element of the volume. Set of simultaneous equations has been solved to get exit gas temperature for two conditions, namely, steady state conditions and dynamic condition.
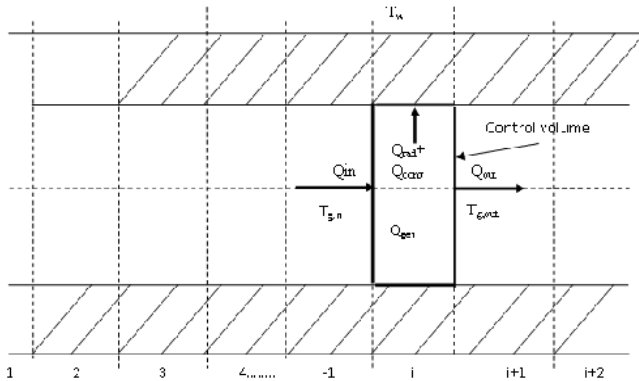

Fig.1 Furnace descritization for calculation of flue gas temperature.

Heat stored in the element = Heat generation – Heat transferred across an element
By applying heat balance equation to i^{th} element in between,

$$\frac{dQ}{dl} = Q_{gen} - Q_{rad} - Q_{conv} \quad \text{.................(1)}$$

$$\frac{d(\dot{m}_{g,i}^{j} C_{pg,i}^{j} T_{g,i}^{j})_f}{dl} = \dot{m}_f \times NCV \times [\exp(-4.6\frac{i-1}{N_f}) - \exp(-4.6\frac{i}{N_f})]$$
$$- Q_{rad} - Q_{conv} \quad \text{...................(2)}$$

where, Flue gas emissivity is calculated by,

$$\varepsilon_g = 1 - (68.2 \times \exp(-2.1 \times \sqrt{C/H})) \quad \text{.......................(3)}$$

Above relation of emissivity is given by 'Ortiz'. It is valid for liquid fuels with C/H weight ratio between 5 to 15. [4].

$$Qrad = \sigma \frac{(2\Pi R_f L_f)}{N_f} \in (T_{av}^4 - T_{wall}^4)_f \quad \text{.......................(4)}$$

$$Q_{conv} = h_{in} \times \frac{(\pi D_f L_f)}{N_f} \times (T_{g,i}^{j} - T_{m,i}^{j})_f \quad \text{.......................(5)}$$

Hence, flue gas outlet temperature is calculated by,

$$T_{g,i+1,f}^{j} = T_{g,i,f}^{j} - \frac{dQ}{(\dot{m}_{g,i}^{j} \times C_{pg,i}^{j})_f}$$
........................(6)

This calculated temperature is applied as a inlet temperature to the next element of descritized furnace. This is done with the help of VBA program. Simulation is done over 500 iterations and by successive substitution method; this temperature is inserted at the place of temperature value of previous iteration for the calculation of temperature in next iteration.

c) Calculations for furnace wall temperature
The changes in energy of the water and metal are the main factors affecting dynamics of the boiler [4].
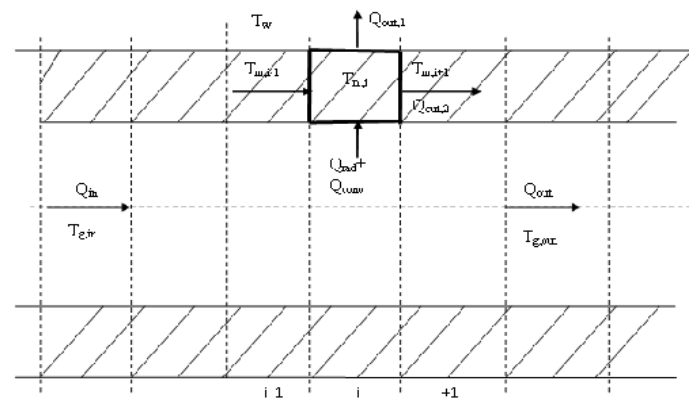

Fig.2 Furnace descritization for calculation of wall temperature.

It is necessary to understand this dynamic behavior of furnace wall temperature to protect boiler from overheating. considering any element 'i' and applying heat balance equation,

$$\frac{dQ}{dt} = (Q_{gen} + Q_{rad} + Q_{conv.}) - (Q_{out1} + Q_{out2})$$
.......................(7)

Q_{gen}, Q_{rad} and Q_{conv} are calculated as in previous case.
Convective heat transfer from furnace wall to water,

$$Q_{out,1} = \frac{(\Pi \times D_f \times L_f)}{N_f} \times h_{out} \times (T_{m,i}^{j} - T_w)_f$$
.......................(8)

Conductive heat transfer from an element 'i' to an element 'i+1' along furnace length is given by,

$$Q_{out,2} = K \times (\pi \times D_f \times t) \times \frac{(T_{m,i}^{j} - T_{m,i+1}^{j})_f}{(L_f / N_f)}$$
...................(9)

Also, Heat stored in the element due to heat transfer through element is given by,

$$\cdots dq = \dot{m}_{m,i}^{j} \times C_{pm,i}^{j} \times (T_{m,i}^{j} - T_{m,i}^{j+1})_f$$

equations (7) and (10) have been solved to get exit temperature of an element 'i' ,

$$T_{m,i,f}^{j+1} = T_{m,i,f}^{j} - \frac{(dQ \times dt)}{\dot{m}_m \times C_{pm,i,f}^{j}} \quad ....(11)$$

Above equation has been solved for all 50 elements of descritized furnace to get furnace wall temperature distribution along length.

d) Internal reversible chamber

Internal Reversible Chamber (IRC) provides passage for flue gases to turn and enter into the convective tubes. This can be modeled similar to the furnace but modeling approach makes difference in both the models. IRC length is very short as compared to furnace length. So, as discussed before, stirred reactor model can be used in this case, which is simpler than plug flow model. As per assumptions made in the model, rate of heat generation and temperature is uniform everywhere and that temperature is assumed to be equal to the flue gas exit temperature. IRC is surrounded by water from all sides.
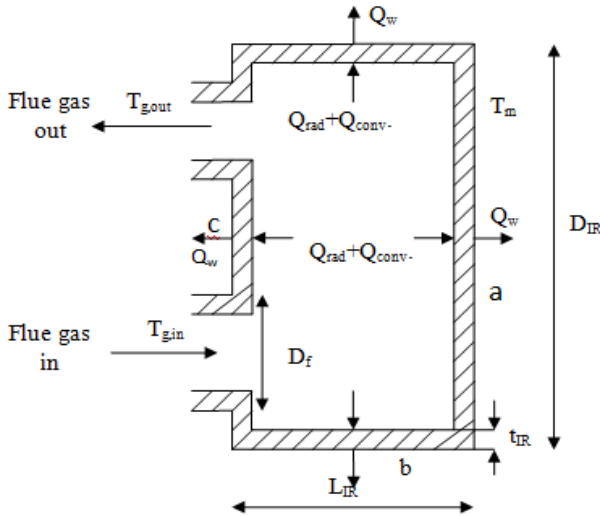

Fig.3 Internal Reversible Chamber

Fig. (3) explains how the heat transfer is taking place from IRC to water. It is cooled by water from all the sides but area through which heat transfer takes place is not same everywhere. One side of IRC is connected to the furnace and other two sides are exposed to water. For the ease of modeling, IRC has been divided in three parts namely, a, b and c as shown in the fig. (3) and respective areas of the three are as follows,

$$A_a = \pi \times D_{IR} \times L_{IR} , \quad A_b = \frac{\pi}{4} \times D_{IR}^2 , \quad A_c = \frac{\pi}{4} \times (D_{IR}^2 - D_f^2)$$

As per assumptions of stirred reactor model,

• $T_{gin,a} = T_{gin,b} = T_{gin,c}$
• Heat generation = 0

e) Calculations for flue gas outlet temperature

General heat balance equation can be written as,

$$\frac{dQ}{dl} = Q_{gen} - Q_{trans} \quad ....(12)$$

$$\frac{dQ_a}{dl} = Q_{gen} - Q_{Conv,1} - Q_{rad,a} \quad ....(13)$$

Similar equations can be write for parts b and c.

Total heat stored per unit length in sides a, b and c is,

$$dQ = dQ_a + dQ_b + dQ_c \quad ....(14)$$

Flue gas outlet temperature can be calculated as,

$$T_{g,out} = T_{g,in} - \frac{dQ}{(\dot{m}_g C_{p,g})} \quad ....(15)$$

This represents IRC flue gas outlet temperature and it is treated as inlet temperature for modeling first convective pass.

f) Calculations for IRC wall temperature

Heat balance equation is,

$$\frac{dQ}{dt} = Q_{g-m} + Q_{m-w} \quad ....(16)$$

$$Q_{g-m} = Q_{rad} + Q_{conv,1} \quad ....(17)$$

$$Q_{Conv,1} = h_{in} \times \frac{\pi D_{IR} L_{IR}}{N_I} \times (T_{g,in} - T_m)$$

$$.........(18)$$

$$Q_{Conv,m-w} = \pi D_{IR} L_{IR} \times h_{out} \times (T_m^j - T_w)$$

$$..........(19)$$

metal wall temperature is calculated by,

$$T_m^{j+1} = T_m^j - \frac{(Q_{in,g-m} - Q_{conv,2}) \times dt}{(m_m \times C_{pm}^j)}$$

$$..........(20)$$

Simulation in Excel/VBA is done over 500 iterations for the calculation of the correct metal temperature. Successive substitution method has been used to solve the equations.

g) Water/Steam side modelling

Modelling of water/steam side becomes very important because of complex heat transfer and mass transfer phenomena. This plays important role in working of controllers used in the boiler. Basically pressure and water level are the main controlling parameters. Apparent rise and fall of water level due to change in load affects adversely on the controller actions. This apparent rise and fall is called shrink and swell phenomena. Actually pressure and water level are not being controlled but flow of feed water and flow of fuel is being controlled which ultimately controls pressure and water level.
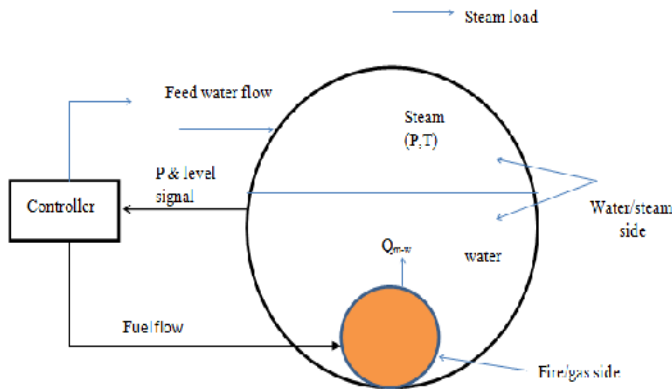

Fig.4 Working of fire-tube boiler through control system

Fig (4) explains the behavior of boiler i.e. heat transfer, mass transfer and working of control elements.

To describe this in the form of mathematics, let us consider boiler at certain conditions (certain P, T, h and quantities of water, steam and bubble). At these conditions, water and steam possesses some properties with their respective values at that pressure and temperature.

Newton-Raphson method has been found effective for such calculation.

Newton Raphson formula can be written as,

$$P_{new} = P_{old} - \left(\frac{f(P)}{f'(P)} \right)_{vapor}$$

..................(21)

As we know, for steam,

H = f(P)……….. (H = enthalpy balance) . ...(22)

Hence, f'(P) = dH/dP

By substituting all values and rearranging equation (21),

$$P_{new} = P_{old} - \left(\frac{H}{dH/dP} \right)$$

...................(23)

This calculation repeats for 500 iterations upto steady state is reached. For new iteration, Pnew is inserted as input pressure and from this, corrected pressure is calculated.

h) Mass balance

When boiler shifts from initial state to next state, steam quantity will have to maintain mass balance by changing rate of combustion and feed water supply to maintain pressure inside the boiler at required level. Hence mass balance equation between these two different conditions can be written as,
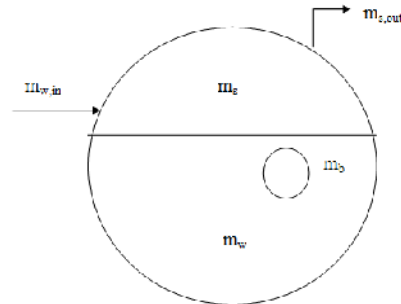

Fig.5 Mass balance in boiler shell

Mass stored in the system = mass going out of the system – mass coming into the system.

also this can be written as,

$$M = \left(m_{s,1} - m_{s,out2} \right) + m_{b,out} - m_{w,in}$$

......…....……… (24)

i) Enthalpy balance

Enthalpy balance calculation plays important role in calculation of pressure. When load on the boiler changes, rate of combustion have to change as per requirement. This will change quantity of heat transfer from flue gas to water which causes change in enthalpies of water and steam present in the shell. Bubble formation and collapse takes place due to this heat addition. All this changes have to capture while developing mathematical model. Following equation gives enthalpy balance when boiler changes from initial state to final state.

$$H = \left(m_{fw} C_{pw} T_{fw} \right) + Q_{m-w} + \left(m_w \times h_{liq} \right)_{in} + \left[(m_s + m_b) \times h_v \right]_{in} - \left(m_{s,out} \times h_v \right) - \left(m_w \times h_{liq} \right)_{fin} - \left[(m_s + m_b) \times h_v \right]_{fin}$$

.....................(25)

This equation gives enthalpy balance value, which is used in Newton-Raphson method for the calculation of pressure.

Where,

H = enthalpy balance (kJ) ,in = initial state, fin = final state, h = enthalpy (kJ/kg), m = mass (kg),fw = feed water

t = time (sec).

III. CASE STUDY

The objective of the case study simulation is to estimate the suitability of the model proposed. The fire tube boiler has simulated using VBA/Excel. Before simulation, all the constants and parameters such as boiler geometry and configuration including PID, valves.

Also heating value of fuel and ambient conditions are set. The simulation starts once the boiler is ready and so the fuel and air are entered following the model. When the convergence is achieved and desired steady state is reached, some changes can be carried out to get the dynamic behaviour of the boiler till new steady state is reached.

As a case study, a 1-Ton boiler has been selected. Table (1) includes the steady state operating conditions of the simulated boiler.

Steady state results

Load = 800 (kg/hr)

Consider boiler is running at load 800 and steady state has reached. At this condition fuel, flow rate to the furnace is almost 59.89 kg/sec. with this fuel flow combustion takes place in the furnace and flue gas produces. Maximum temperature reached in the furnace, which called flame temperature, is almost 1178.505 0C at steady state. Flue gas passes over furnace length, transferring heat to the furnace wall. Steady state values of all the parameters have given in following table.

Table 1. Steady state operating conditions of the case study

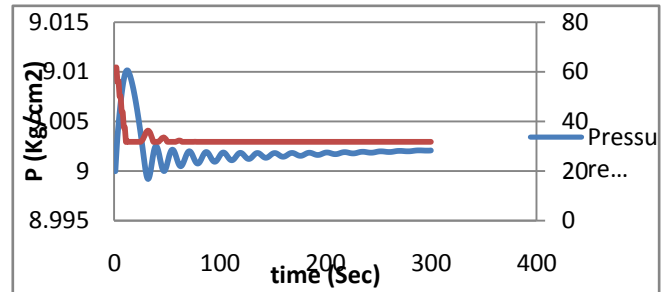| Parameters	Values
Steam pressure	9.0 kg/cm2
Steam flow rate	800 kg/hr
Water volume	7.0 m3
Feed water flow rate	882 kg/hr
Feed water temperature	800C
Fuel flow rate	59.89 kg/hr

Sudden load change from 800 to 500 kg/hr

Fig.6 Pressure and fuel flow dynamics when load changes from 800 Kg/hr to 500 kg/hr.

Figure 6 shows that, when there is sudden decrease in the load from 800 to 500 kg/hr, there is sudden increase in the steam pressure in the boiler. As soon as pressure increases, signal is transmitted to the PID and it generates instruction to reduce the fuel flow and sends it to the fuel control valve. Control valve regulates the fuel flow and reduces it from 59.89 kg/hr to 31.75 kg/hr. as fuel flow which is generally called as rate of combustion reduces, temperatures of flue gases also reduces and heat transfer to the water from flue gas also reduces and ultimately steam generation reduces by maintaining pressure at desired value. This process takes some time because signal transmission, instruction generation, valve operations and heat transfer process happen one after other. From figure 6, it can be noted that initially there are fluctuations in the pressure and fuel flow values and after almost 5 minutes both reached to steady state.
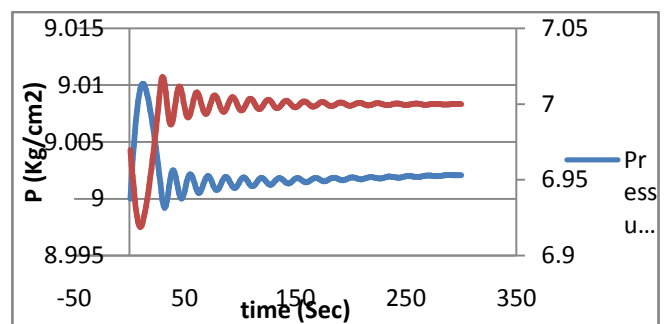

Fig. 7 Pressure and water volume dynamics when load changes from 800 kg/hr to 500 kg/hr.

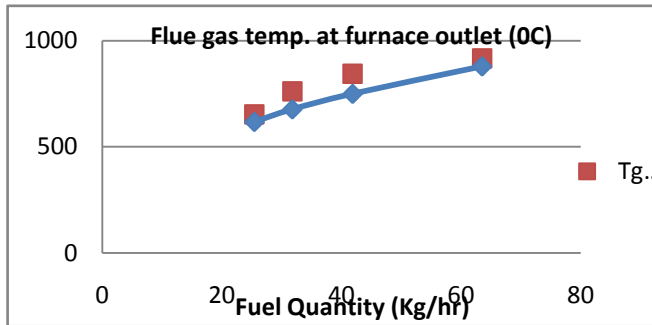**Validation with experimental results**

Fig.8 Experimental vs. modeling results for flue gas temperature at furnace outlet.

Figure (8) shows compareson of modeling results against experimental results. When load has varied from 40% to 100%, fuel quantity changes correspondingly. At 40% load, fuel quantity is almost 25.4 kg/hr and with this quantity, combustion takes place. Figure shows comparison of modeling and experiental values of flue gas temperature at furnace outlet. With 25.4 kg/hr fuel flow, furnace exit temperatures obtained with modeling and with experiment do not vary much but as fuel flow, increses at 60% load to almost 33 kg/hr, significant difference in both values can, observed. It is mainly due to assumptions made in the modeling. Combustion pattern also affects the results. It can observe from the graph that, as load on the boiler increases, fuel quantity increases to maintain the desired pressure and hence, flue gas temperature at furnace outlet increases.
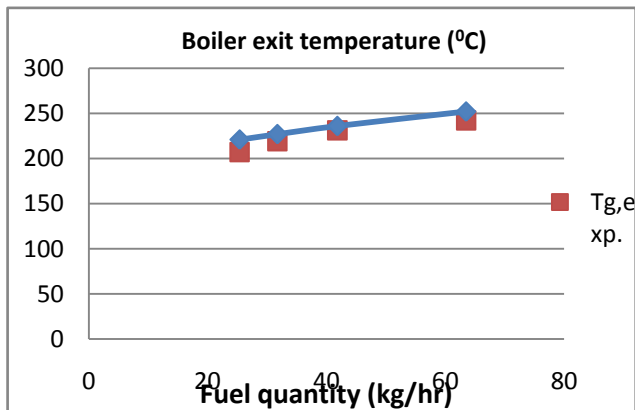

Fig.9 Experimental vs. modeling results for flue gas temperature at boiler exit.

Boiler exit temperature is the temperature at the exit of the second convective pass of the boiler. Figure 9 shows the comparison of flue gas outlet modelling result with corresponding experimental results. Values obtained by both the approaches seem very close to each other. Figure shows variation of boiler exit temperature at different fuel quantities. Fuel quantity is almost 25.4 kg/hr at 40% load and varied to 63.5 kg/hr at full load and corresponding boiler exit temperatures have checked with both the approaches.

CONCLUSION

A complete dynamic model of a full-scale fire-tube boiler has been developed based on the mass, energy. Two parts are distinguished in fire-tube boilers:

1) The fire/gas side and

2) The water/ steam side.

Also on water/steam side, module for bubble formation has been introduced which gives better idea of level fluctuation. A case study has been simulated using a 1Ton fire-tube boiler and dynamic performances predicted by the model are in good qualitative agreement with experimental data.

Error in the flue gas temperature at the outlet of the boiler comparing with experimental value is almost 4%.

Error in the fuel firing rate (kg/hr) comparing with experimental value is almost negligible.

REFERENCES

1. Kumar Rayaprolu, Boilers for poewer and process, CRC press, London, Vol.13.

2. Kim Sorensen,Thomas Condra, Neils Houbak, Modeling, Simulating and Optimizing boiler heating surfaces and evaporator circuits.

3. K. J. Astrom, R. D. Bell, Drum Boiler Dynamics, In IFAC 13th world congress, San Francisco, CA, 1996.

4. F. J. Gutierrez Oritz, Modeling of fire-tube boilers, Journal of Applied Thermal Engineering 31(2011), 3463-3478.

5. Shuaibu Ndache Mohammed, The investigation of furnace operating characteristics using the long furnace model, Leonardo Journal of Sciences, ISSN 1583-0233, p.p 55-66, Jan.-July-2007.

6. H Verbanck, Development of a mathematical model for water-tube boiler heat transfer calculations, 1997.

Nomenclature

Q - Heat transfer, W

ρ - density, Kg/m3

Cp - Specific heat, kJ/kg ^{0}C

T - temperature, ^{0}C

H - enthalpy, kJ/kg

m - mass, Kg

K - Conductivity, W/m^{0}C

h - Heat transfer coefficient, W/m2 ^{0}C

L - Length, m

d - Diameter, m

t - thickness, m

γ - Specific gravit

Subscripts   **Superscripts**

  i - No. of section   j - Time (sec)

  b - Bubble

  s - Steam

  m - metal

 f – Furnace

● ● ●

Effect of helix parameter modification on flow characteristics of CIDI diesel engine helical intake port

[1]Kunjan Sanadhya, [2]N. P. Gokhale, [3]B.S. Deshmukh, [4]M.N. Kumar, [5]D.B. Hulwan
[1][2][3][4] Kirloskar Oil Engines Ltd., Pune, India, [5] Vishwakarma Institute of Technology, Pune, India
[1]kunjan.sanadhya@kirloskar.com,[2]nitin.gokhale@kirloskar.com, [3]bhalchandra.deshmukh@kirloskar.com,
[4]m.kumar@kirloskar.com, [5]dbhulwanvit@gmail.com

Abstract- **This project work involves experimental investigation of helical inlet port flow characteristics for cylinder head of Direct Injection (D.I) diesel engine. The average flow coefficient and swirl number is obtained using a paddle wheel test bench. Intake port helix parameters, i.e., distance between peripheral side wall and valve axis 'D$_p$', width of helical section parallel to valve axis 'W' and initial width of the helix 'W$_h$' are measured for different flow boxes for selected different bore and stroke engines. These parameters are modified and detailed analysis has been done to establish the effect on swirl number and average flow coefficient. The second part of work focused on the Computation Fluid Dynamics (CFD) to study flow velocity, flow distribution inside cylinder and to analyze effect of helix parameter change. The experimental study of combined effect of helix parameters, 'W', 'W$_h$' and 'D$_p$' indicates that this modification can be initiated for improving flow characteristics if change required in average flow coefficient is small as compared to higher amount of change required in swirl number. The CFD analysis with this modification also shows improvement in swirl generation and flow distribution.**

Key words- **Average Flow Coefficient, Diesel Engine, Helical Port, Paddle wheel, Swirl Number**

I. INTRODUCTION

Air motion into the cylinder during intake stroke of an internal combustion engine is one of the important factors, which govern the performance of an engine. Swirl is the rotation of charge about cylinder axis and it is used in diesel engines to control air-fuel mixing. Several research studies related to swirl enhancement in IC engines reported that swirl facilitates mixing of air fuel mixture and increases the combustion rate. Furthermore, a high swirl is also not desired, as kinetic energy for the flow is obtained at expense of a reduced volumetric efficiency. Optimum swirl can be created by optimum design of the intake port. An optimal swirl ratio is not only good for optimum combustion, but also for an optimal emission reduction [2].

Techniques like paddle wheel anemometer and torque meter are commonly used for steady state swirl measurement [5] and also laser doppler anemometry is used by many authors for study of in-cylinder bulk flow and turbulence structure [4]. The steady state flow analysis helps to find variations in different non-dimensional parameters such as flow coefficient and swirl ratio for various valve lifts. The test results available as comparative ratios, are very useful for obtaining very good approximation of actual engine conditions and for development work on helical inlet

valve ports. This research work is carried out for helical intake ports of five DI diesel engines by using paddle wheel anemometer technique.

Various port modification techniques has been adopted by various authors to improve the flow characteristics of helical intake ports like throat machining [6] and changing parameters like valve cone angle [1], port position relative to cylinder [5], throat ceiling height [5], inlet centre distance [1], transition angle , helix slope angle and bottom slope [5]. In this research work, effect of varying helical parameters i.e. distance between peripheral side wall and valve axis, width of helical section parallel to valve axis and initial width of the helix has been studied. These parameters are converted to non-dimensional form to compare the effect on all flow boxes. The effect of these parameters was studied for all the five experimental flow boxes and a trend is established which can be used to achieve required flow characteristics of any diesel engine helical port.

CFD as a tool can acquire a large amount of information which is unable to gain in experiments such as velocity field and flow field [3][4]. The simulation results can be analyzed in terms of distribution of in-cylinder swirl during intake process [5]. In this research work, velocity field and flow distribution was studied using CFD simulation software. At

the end velocity field and flow distribution with and without modification were also compared.

II. EXPERIMENTAL SETUP

A paddle wheel swirl test rig was used to determine swirl number and flow coefficient. The picture of the test rig is shown in fig. 1. The experimental work was carried out on helical intake port models, normally known as flow box. "A", "B", "C", "D" and "E" is the nomenclature adopted for five flow boxes in this research work. The table. I show engine details of flow boxes used for test bench experimentation.

All flow boxes used for this experimental work were cylinder head models of engines with two valves per cylinder. For experimentation separate liners of bore sizes of table. 1 with mounting flanges was used and the test setup does not include piston.

Table. I- Flow box engine details.

Engine Name	A	B	C	D	E
Bore	110	114.3	87.5	96	87.5
Stroke	125	116	80	112	80
Valve Seat Diameter	42.0	44.5	35.3	37.8	31.7
Connecting Rod Length	216	231.9	148	187	148

Valve assembly of the same engine type was mounted on the flow boxes and that flow box was placed on liner. Both liner and flow boxes were clamped using studs and nuts. Arrangement to change valve lift by measured amount using micrometer was also prepared.

A paddle wheel is normally mounted at a distance equal to 1.75 times bore diameter because the time taken for the charge to travel from the valve to 1.75 bore diameter position along the flow bench cylinder is equivalent to a time between maximum intake valve lift and top dead center firing in the running engine [6]. The paddle wheel diameters, length and height were taken as some ratio of bore and same ratio was used for all the trials. Also same vane thickness was used while preparation of paddle wheels.

Air is sucked by the blower through the port, over the valve, cylinder liner and surge tank as shown in fig. 1. This creates a vacuum below the valve.

The method used for experimentation is commonly used for calculating average or mean flow coefficients from the results of steady state flow tests conducted with paddle wheel method [5]. Typically the procedure used is based on the instantaneous measurement of mass flow rate, paddle wheel rotations per minute and pressure drop across the port at different valve lifts. Based on these measurements dimensionless flow coefficient and swirl ratio was computed at all valve lifts using equation (2) and equation (5). Since the swirl ratio measured in steady-state flow tests varies depending on valve lift, average swirl ratio during intake stroke can be defined as value found by integrating the angular momentum induced at each valve lift. The average flow coefficient during intake stroke can also be defined in the same way. Formulas used are included in Appendix.

Fig. 1 Experimental setup used for experimentation
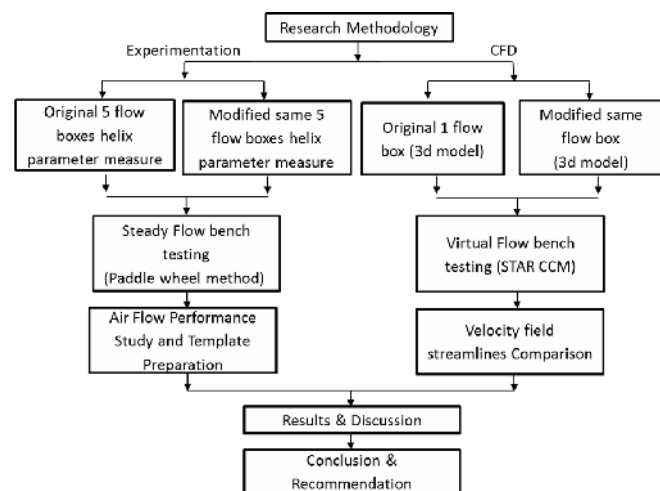
III. METHODOLOGY

Fig. 2 Research methodology

Fig. 2 explains the methodology used for this research work. The experimental part of this research work has been focused on measuring swirl ratio and flow coefficient of five flow boxes at 13 valve lifts for original as well as modified flow boxes. After the test of original flow boxes, same flow boxes were modified and tested. Average flow coefficients and swirl number was measured from experimental outputs. The original and modified helix parameters were measured and normalized with valve diameter of engine to which the flow box belongs. The average flow coefficients and swirl number were compared for flow boxes before and after modifications using these normalized parameters. The CFD simulation was also carried out with intake port 3d model of one engine from experimental engines of table. I to see the effect of helix parameter change on velocity profiles and flow patterns by using mass flow rate from experimentation.

IV. GEOMETRY PARAMETER MODIFICATION

Three helix parameters, specifically, distance between peripheral side wall and valve axis 'D_p', width of helical section parallel to valve axis 'W' and initial width of the helix 'W_h' shown in Fig. 3 have been modified on all flow boxes. These parameters were modified by adding material (known as putty) as shown in table. II.
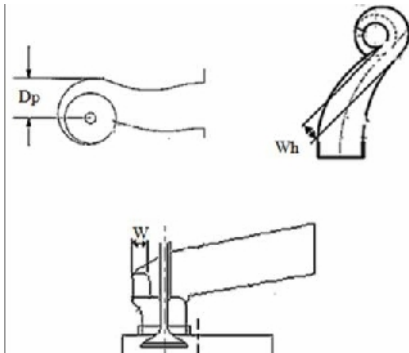

Fig. 3 Sketch of parameter 'D_p', 'W' and 'W_h'.

Table. II Terminology used for the original and modified helix parameters of flow box "A"

| A Original Flow Box | |
| A1 Flow box with modified D_p W, and W_h | |

All these parameters are related to helix and hence were modified together to retain helix shape of the helical intake port. The modification done by this method can be undone unlike methods similar to polishing or material removal [2] from flow box.

In this paper, "A" is used as a representation for original flow box and "A1" is used for modified flow box representation as explained in table. II. Similar nomenclature is used for flow boxes "B", "C", "D" and "E".

V. GEOMETRY PARAMETER NORMALIZATION

The helix parameters 'D_p', 'W' and 'W_h' were measured for all flow boxes before and after modification. These parameters were then normalized with respect to valve seat

diameter of that particular flow box or equivalent engine. Table. III and Table. IV lists the normalized helix parameters of tested original and modified flow boxes.

Table. III Normalized parameters of original flow boxes used for trial

S.No.	Normalized Original parameters	A	B	C	D	E
1	D_p/d_v	0.69	0.73	0.71	0.74	0.74
2	W/d_v	0.34	0.36	0.16	0.29	0.31
3	W_h/d_v	0.44	0.47	0.30	0.34	0.49

Table. IV Normalized parameters of modified flow boxes used for trial

S.No.	Normalized Original parameters	A1	B1	C1	D1	E1
1	D_p/d_v	0.65	0.66	0.65	0.64	0.68
2	W/d_v	0.20	0.28	0.08	0.19	0.15
3	W_h/d_v	0.29	0.39	0.24	0.24	0.43

This normalization technique allows eradication of engine size effects from data and can be used to compare measured dimension of flow box of different engines . In this research work, these normalized parameters were used to study the effect of helix modification on average flow coefficient and swirl number calculated using experimental results .

VI. COMPUTATIONAL FLUID DYNAMICS

Model details and boundary conditions

Three dimensional model including cylinder, valve and helical port was used for the study of velocity field and flow streamline in engine "D". After importing model in software, it was split to separate the boundaries in outlet, cylinder, valve, port and inlet boundaries. Surface and volume meshing was done for the model with 13 mm valve lift. A steady flow case with incompressible working fluid was considered. As the experimental setup does not include piston, no piston was used for CFD model also and bottom of the cylinder was kept open and K-epsilon turbulence model was used. Constant mass flow rate at 13 mm valve lift obtained from experimental data was used as inlet boundary condition and static pressure of 0 Pa was used as boundary condition at outlet open end.

Model Validation

Using above boundary conditions, mass flow averaged pressure at inlet and outlet were obtained from the analysis. Equation (3) was used for flow coefficient measurement. Where, actual mass flow is taken as the mass flow used for inlet boundary condition which is same as the experimental mass flow result, while theoretical mass flow was measured using equation (4). Valve seat diameter was used same as that of engine "D".

 The flow coefficient obtained from above calculation was 0.51 while the flow coefficient obtained by experimentation for the same engine was 0.49. The flow coefficient result of CFD model and experimentation differs by 4 % which is acceptable. Thus, as the flow coefficient is similar to flow coefficient from experiment, the flow velocity field and flow streamlines plots inside the cylinder which are not obtained in the experiment can be studied using this method.

VII. RESULTS AND DISCUSSION

With the test bench data at different valve lifts swirl and flow coefficients was calculated for all flow boxes from equation (1) and equation (3) provided in the appendix and it was observed that increase in swirl ratio was significant at both higher and lower valve lifts while reduction in flow coefficient was less and observed only at higher valve lifts. Also, swirl number and average flow coefficient were calculated for all flow boxes and effect of changing the helix parameter on these flow characteristics was studied. These parameters were changed together as shown in table. II to maintain continuity of helical shape, but the effect of reduction of these normalized parameters was plotted individually for all parameters. Following section is divided in two parts. In first part the effect of helix parameter change on average flow characteristics is depicted while the second part depicts the effect of helix modification on velocity field and flow distribution using CFD.

Effect of helix parameter change on average flow characteristics

In modified flow box area reduction in the region of helix increase air velocity as compared to original flow box and air is forced to enter the cylinder liner with higher velocity and higher density.

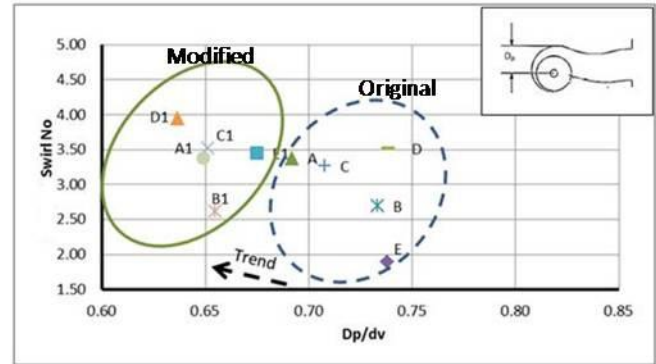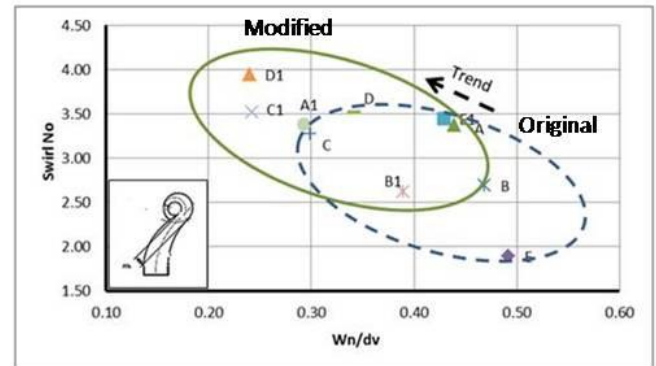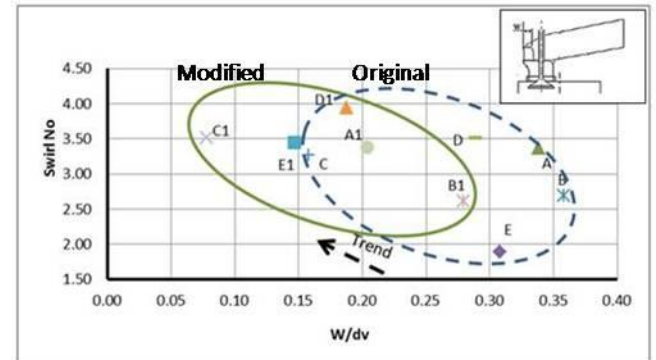*Effect on Average flow coefficient*

As shown in fig. 4, fig. 5 and fig. 6 the calculated average flow coefficient is plotted against the normalized parameters from table III and IV. It was observed that all the flow boxes followed same trend where average flow coefficient reduced with reduction of parameters 'D_p', 'W_h' and 'W'.
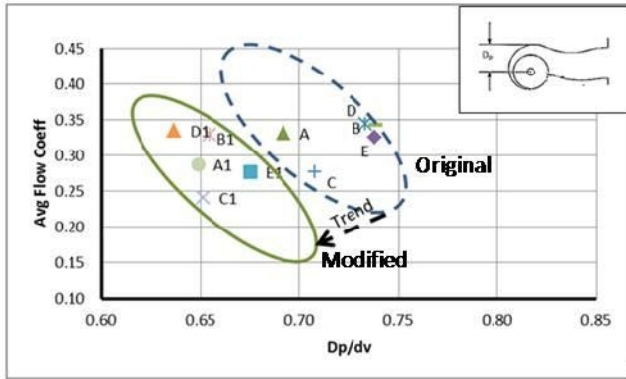
Fig. 4 Average Flow Coefficient Vs. D_p/d_v
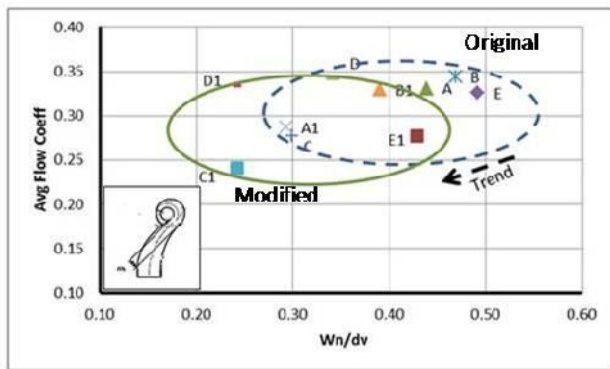
Fig. 5 Average Flow Coefficient Vs. W_h/d_v
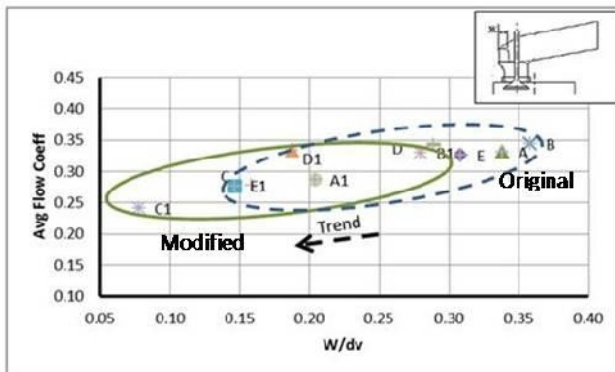
Fig.6 Average Flow Coefficient Vs. W/d_v

Effect on Average Swirl Ratio

Fig. 7, 8 and 9 shows that with 'D_p', 'W_h' and 'W' reduction, swirl number reduces. These parameters change the helical component of swirl. When helical component of swirl increases the swirl ratio of that port also increases at all valve lifts [1].

Fig. 7 Swirl Number. Vs. D_p/d_v

Fig. 8 Swirl Number. Vs. W_h/d_v

Fig.9 Swirl Number. Vs. W_h/d_v

The data from present study illustrates that average flow coefficient reduces by same percentage as that of change in parameter while the swirl number increases by double percentage. This outcome is listed in table V. As the average flow characteristics are derived from flow characteristics at each valve lift, little increase in average flow coefficient and significant increase in swirl number is observed because as per experimental data increase in swirl ratio was significant at both higher and lower valve lifts, while reduction in flow coefficient was observed only at higher valve lifts.

Table. V Change in average flow coefficient and average swirl number by helix parameters modification

Helix Modification	%
D_p/d_v	(-)
W_h/d_v	(-)
W/d_v	(-)
Average Flow Coefficient	(-)
Average Swirl Ratio	(+ +)

B. Effect of helix modification on velocity field and flow distribution by CFD

The velocity field and flow distribution were studied using CFD simulation software. The CFD simulation results can be analyzed in terms of distribution of in-cylinder swirl during intake process [5]. As previously discussed the analysis was carried out for engine "D" and at 13 mm lift only. The fig.10 shows that flow velocity was increased after modification. Also swirl generation and swirl distribution around the cylinder was improved as shown in fig.11, fig.12 and fig.13. In fig.11 after modifications the velocity of streamlines just below the valve was reduced and the distribution inside the cylinder was improved as marked by arrow which shows that tangential velocity of air entering cylinder liner has increased and axial velocity has reduced.

Fig. 11 Side view comparison of flow field for original and modified helix shape at 13 mm lift.

Fig. 12 Bottom view comparison of flow field for original and modified helix shape at 13 mm lift.

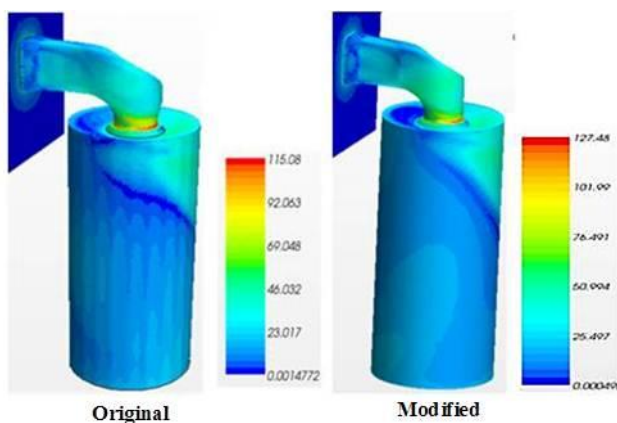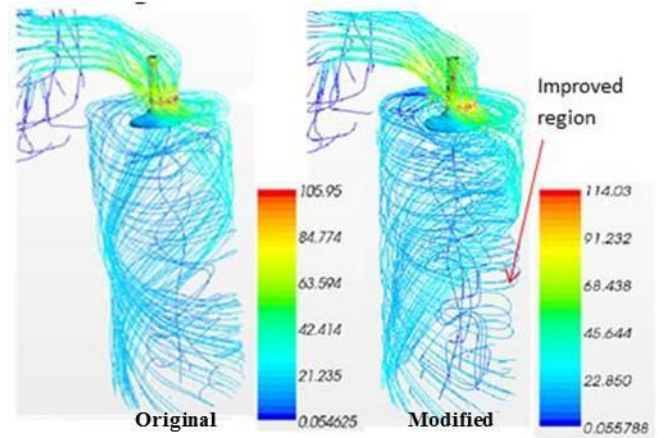

Fig. 10 Comparison of velocity field for original and modified helix shape at 13 mm lift.

Fig. 13 Top view comparison of flow field for original and modified helix shape at 13 mm lift.
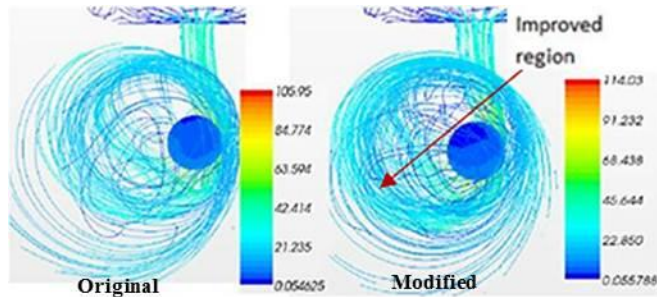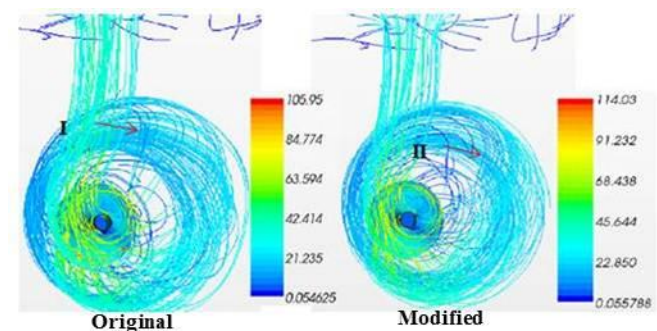
The fig.13 explains that streamlines have shifted from position I to position II which means that more streamlines follows the cylinder wall and swirl is generated with better efficiency after modification.

Thus, as per CFD flow analysis, it is revealed that with helix parameter modification velocity increases and also the streamlines are enforced to follow the cylinder wall and the swirl is generated with better efficiency.

CONCLUSION

As per this research work, helix modification is recommended to obtain the required flow characteristics, if change required in average swirl ratio is approximately double than opposite change required for average flow coefficient for a CIDI diesel engine cylinder head intake port. CFD analysis can be used to determine flow coefficient with approx 4 % variation from experimentation data. Both experimental and CFD analysis depicted that with helix parameter modification axial velocity component reduces and tangential velocity component increases resulting in better swirl generation. Also, CFD analysis has clarified that velocity near valve seat increases and the streamlines are enforced to move towards cylinder wall with helix modification which was difficult to explain from experimentation.

ACKNOWLEDGEMENTS

REFERENCES

[1]   Shuisheng JIANG et al., "Parameter Analysis of Diesel Helical Intake Port Numerical Design", Energy Procedia 16 (2012) 558– 563

[2]   Mohd Taufik Bin Abd Kadir, "Intake Port Flow Study on Various Cylinder Head Using Flow bench", University Malaysia Pahang

[3]   Henk Krus, Cyclone Fluid Dynamics B.V., Waalre, "Numerical simulation and experimental verification of DI diesel intake port designs", Presented at 4th Int. Conf. on Vehicle and Traffic Systems Technology Strasbourg,16-18 June 1993

[4] Toyoshige et al., "Evaluation of CFD Tools Applied to Engine Coolant Flow Analysis", Mitsubishi Motors Review No.16, 2004

[5]   Jun-ichi Kawashima et al., "Research on a Variable Swirl Intake Port for 4-Valve High-Speed DI Diesel Engines", SAE 982680, Nissan Motor Co., Ltd.

[6] Nigel F. Gale, "Diesel Engine Cylinder Head Design: The Compromises and the Techniques", SAE 900133,Southwest Research Institute, San Antonio, Texas

DEFINITIONS/ABBREVIATIONS

CI	Compression Ignition
DI	Direct Injection
d_v	Valve seat diameter
D_p	Distance between peripheral side wall and valve axis
W	Width of helical section parallel to valve axis
W_h	Initial width of the helix

APPENDIX

Swirl Ratio

It is defined as the ratio of anemometer speed to engine fictitious speed as shown by equation (1).

$$\frac{n_D}{n} = \frac{n_D \rho V_h}{30 \dot{m}}$$

(1)

Where,

n_D =anemometer speed[min-1]

n = engine speed [min-1]

$\dot{m}$ = mass flow

V_h= cylinder displacement

ρ = air density

Swirl Number or Average Swirl Ratio

It is obtained by integration over crank angle between TDC to BDC considering valve lift and piston speed. Equation (2) is commonly used for calculating average swirl ratio from the results of steady state flow tests conducted with paddle wheel method [5].

$$\left(\frac{n_D}{n} \right)_m = \frac{1}{\pi} \int_0^\pi \frac{n_D}{n} \left(\frac{c(a)}{c_m} \right)^2 d\alpha$$

(2)

Where,

c(a) = actual piston speed

index m = mean

Dimensionless flow coefficient

It is defined as the ratio of actual mass flow over a theoretical mass flow; refer to equation (3). Actual mass

flow value is obtained from the measurement of mass flow rate for a fixed pressure drop Δp across the port at different valve lift using a steady air flow or it is a measure of the pressure loss introduced by the port/valve combination. While, theoretical mass flow is calculated from the fictitious velocity in the open seat area $(\pi/4)*d_v^2$ at an equal pressure drop assuming a flow free of losses [3], refer equation (4).

$$\mu\sigma = \frac{\dot{m}}{\dot{m}_{th}}$$

(3)

$$\dot{m}_{th} = z\frac{dv^2\pi}{4}\rho\sqrt{\frac{2\Delta p}{\rho}}$$

(4)

Where,

z = number of valves

d_v = inner seat diameter

Average Flow Coefficient

It is computed by integration over the crank angle between TDC and BDC considering valve lift and piston displacement. Equation (6) is commonly used for calculating average or mean flow coefficients from the results of steady state flow tests conducted with paddle wheel method [5].

$$(\mu\sigma)_m = \frac{1}{\sqrt{\left(\frac{1}{\pi}\int_0^\pi \left(\frac{c(\alpha)}{c_m}\right)^3 \frac{1}{(\mu\sigma)^2}d\alpha\right)}}$$

(5)

● ● ●

Comparative Analysis of Fixed Base and Base Isolated Building with Lead Core Rubber Bearing

[1]Shrijit S Menon, [2] P.R.Barbude

[1] P.G. Student, Department of Civil Engineering, DattaMeghe College of Engineering, Mumbai, Maharashtra, India,
[2]Assistant Professor, Department of Civil Engineering, Datta Meghe College of Engineering, Mumbai, Maharashtra, India,
[1]Shrijit_menon89@yahoo.com, [2] prbarbude@yahoo.com

Abstract- **Nowadays Base Isolation is widely accepted as a protection system for structures against seismic threats. Its basic principle is to isolate the superstructure from the substructure and to have a flexible material in the horizontal plane that is capable of preventing energy flow into the superstructure, in other words here the structure is decoupled from the earthquake ground motions by providing separate isolation devices between the base of the structures and its foundation thereby shifting the fundamental period of the structure out of the range of dominant earthquake energy frequencies and prevent the superstructure from absorbing it.The aim of this study is to provide a brief overview of the seismic isolation technology that is rapidly becoming more prevalent in the seismic design of building structures and a parametric comparison on the basis of Dynamic Analysis i.e. Response Spectrum Analysis between Fixed Base and Base Isolated Structure using Lead Core Rubber Bearing is made. For comparison purpose, a G+4 story RC Model is considered and the analysis is conducted with the help of Midas Gen Software.**

Key words- **Base Isolation, Lead Core Rubber Bearing, Decoupled, Hysteric Behavior, Response Spectrum Analysis.**

I. INTRODUCTION

The seismic isolation structures from ground motions is already a well-known method. During earthquake it provides a high reliability and protection from damages than an earthquake resistant system. Seismic isolation technology allows converting weak and vulnerable buildings to practically earthquake proof buildings by reducing the transfer of the ground motion effect to the building without interruption of the functional operations of it.

Seismic isolation commonly referred to as base isolation is a construction method for protecting buildings, in which the building and ground are separated by an isolation system to reduce the transfer of seismic vibrations through the structure. It reduces the seismic forces and changes it to a slow & relatively low vibration, so not only the building, but also everything inside is protected.

In recent year base isolation has become an increasingly applied structural design technique for important structures in highly seismic zones. Many structures have been built using this approach and many others in the design phase or under construction. Principle of base isolation can be well explained using response spectrum analysis, as acceleration is one of the most important factor affecting the response of a structure. The base isolation system is inherently nonlinear i.e. it possess material or geometrical or both nonlinearity with hysteretic behavior. For general design purpose an equivalent linear approach is followed in the form of response spectrum analysis for simple understanding.

II. BASIC PRINCIPLE OF BASE ISOLATION

In seismic base isolation, a flexible mount is inserted at the bottom level of the structure. This mount increases the damping and the flexibility of the structure in the horizontal direction. This increases the time period of the structure. Thereby by base isolation, a reduction in seismic demand is achieved.

Generally Base isolation techniques follow two approaches. In the first one, a layer of low lateral stiffness is introduced between the structure and foundation. With this isolation layer, natural time period of structure is lengthened than its fixed base period.

The second approach uses sliding elements between foundation and base of the structure. The shear force transmitted to the structure across the isolation interface is kept under control by keeping the coefficient of friction as low as possible.
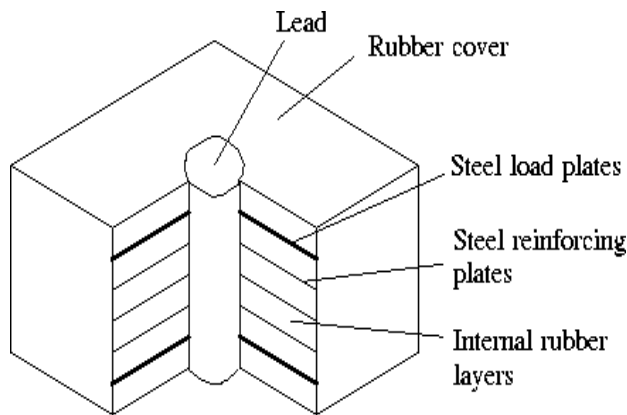
III. LEAD RUBBER BEARING (LRB)

The Lead-rubber Bearing Isolator is a type of elastomeric bearings. It is probably the most economical isolator. It comprises of a rubber pad reinforced with laminated steel sheets as shown in Figure-1, circular lead core is inserted at

the center of the rubber pad. The pad is then attached to two steel plates at both extreme faces as interface to connect the isolator with the structure.

The rubber used in these isolators consists of the same elastomeric material used in bridges with special specifications to accommodate seismic requirements. The rubber in this case serves as a soft material that provides soft support for isolation purposes. The rubber itself is not a good energy dissipater since it is a purely elastic material. Owing to low damping in rubber compounds that is in adequate to control the displacements of the isolation system, researchers developed a system that uses a cylinder of lead enclosed is an elastomeric bearing. The function of lead plate is primarily to dissipate energy while the laminated rubber bearing provides the lateral flexibility.

Figure -1: Lead Core Rubber Bearing (LRB)

As a material, lead has moderate stiffness and large capacity of energy dissipation, therefore it is considered ideal for this system to achieve three important goals. First, it limits large displacements due to lateral forces under normal conditions due to its elastic stiffness. Second, it yields under seismic excitations at low force levels to activate the function of the rubber as an isolator. Third, it serves as a damper due to its large energy dissipation capacity.

IV. LITERATURE REVIEW

Many technical papers from various construction journals from India and abroad are studied to understand the necessity of this study and its importance in view of present scenario in construction industry. Very limited work has been done in India on this subject. However, detailed study has been done in Japan, New Zealand and other countries on Base Isolation and its pros and cons.

[Kelly, 1986] has compiled a review of Isolation Devices used and studied between 1980 to 1984.Many Scientists have studied the dynamic behaviors of base isolated structures under earthquakes using different devices for seismic isolation. A comprehensive study on application of isolation devices for practical use was put forward by [Skinner, 1993].

In general most isolation systems are nonlinear in terms of force displacement relationship; however a linear analysis of base isolated structure using simple model allows us to study the dynamics of the system more efficiently [Chopra, 2002].The nonlinear behavior of the isolation systems can be effectively expressed as Bilinear [Pradeep Kumar, 2007] also the 3D dynamic analysis procedure of base isolated Structure is discussed by [Deb, 2004].

1. modelling and description of structural system

The current study is aimed at studying the effectiveness of base isolation for a simple reinforced concrete structure. In order to make a parametric comparision between a Fixed & Base Isolated Structure, a Five Story reinforced building has been modelled and analysed using structural analysis software Midas-Gen.

Building Features:

1.	Type of Structure	Multi-story Reinforced Concrete frame
2.	Earthquake Zone	IV
	Response reduction factor	3
	Importance factor	1.5
3.	Layout & Elevation	As shown in Figure no 2,3
4.	Number of stories	5 (G + 4)
5.	Ground story height	3.0m
6.	Floor-to-floor height	3.0 m
7.	Live load	3 KN/m2
8.	Materials	M 30 and Fe 500
9.	Seismic analysis	Response Spectrum Analysis
10.	Design Philosophy	Limit state method conforming to IS 456 : 2000 + IS 13920

11.	Size of columns	400 X 400 mm
12.	Size of Beams	300 X 600 mm
13.	Slab Thickness	160 mm
14.	Structural Analysis	Midas Gen 2015 version 11

Isolator Properties

Vertical Stiffness (Kv)	814 KN/mm
Horizontal Stiffness (Kr)	1.1 KN/mm
Equivalent Stiffness (Ke)	1.89 KN/mm
Yield Force(Q)	315 KN
Post Yield Stiffness Ratio	0.1
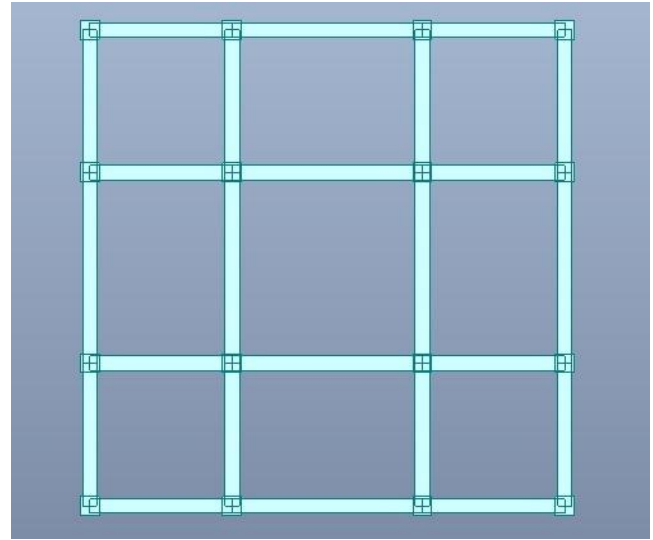
Figure-2:Typical Floor Plan

Figure-3: Elevation

V. RESULTS AND DISCUSSION

Response Spectrum Analysis

In case of seismic loading, the most popular way of quantifying the demand is by using Response Spectrum. Response Spectrum is a plot of spectral parameters (acceleration, velocity or displacement) versus the time period for some given level of damping. These spectral parameters 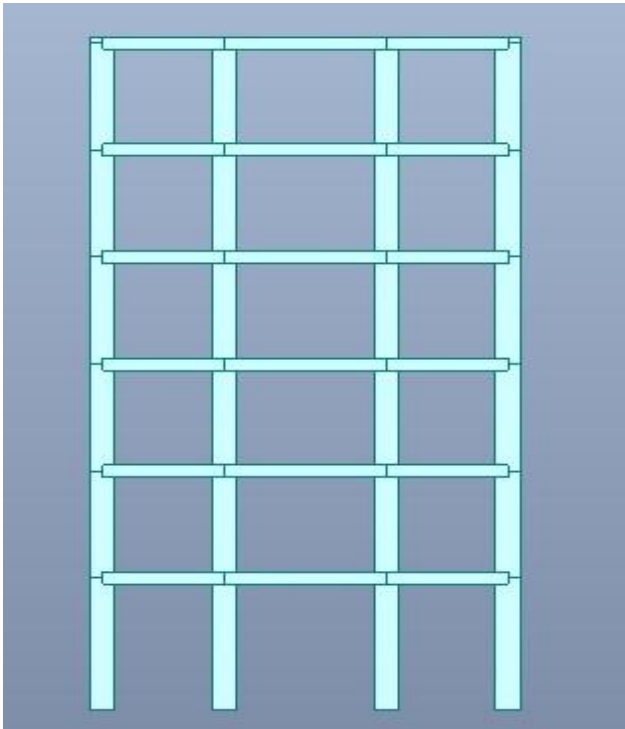are used further to calculate the demand on the various structural components In the present work building with LRB having bilinear force deformation behavior is used. The results are presented in comparative manner.

Table-1: Time Period

Mode	Fixed Base Response Spectrum Time Period (Sec)	Base Isolated Response Spectrum Time Period (Sec)
1	0.7919	1.6802
2	0.7919	1.6784
3	0.6631	1.4476
4	0.2569	0.3432
5	0.2569	0.3416
6	0.2154	0.2803

7	0.1447	0.1659
8	0.1447	0.1645
9	0.1241	0.1417
10	0.1009	0.1112

Here, from the results of Time Period and Frequency it is quite clear that by providing base isolators the time period increases which aids us in reducing the intensity of a seismic threat.
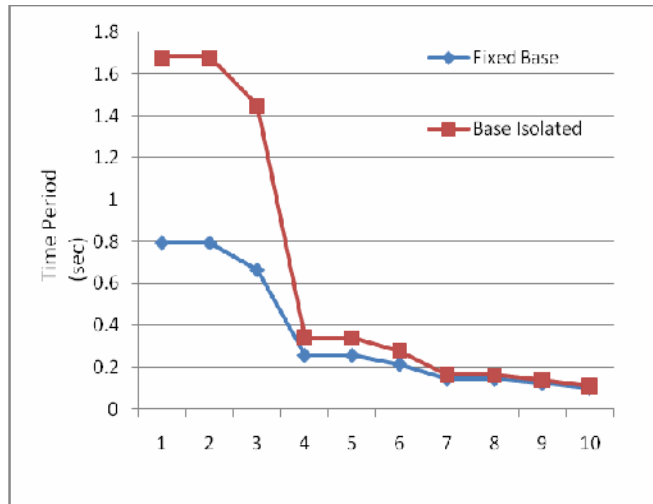
Figure-4: Time Period vs Mode

From the Graph it is clearly visible in case of base isolated model the time period for the first 3 major Mode shapes has increased predominately when compared to the fixed base one. Hence the primary function for which we introduce base isolator i.e. to lengthen the time period is served

Table-2: Frequency

Mode	Fixed Base Response Spectrum frequency (rad/Sec)	Base Isolated Response Spectrum frequency (rad/Sec)
1	7.9345	3.7396
2	7.9345	3.7435
3	9.4759	4.3404
4	24.453	18.3057
5	24.453	18.3917
6	29.1709	22.4139
7	43.4314	37.8817
8	43.4314	38.1907
9	50.6277	44.3522
10	62.2475	56.5289

Table-3: Story Shear

	Fixed Base	Base Isolated	Fixed Base	Base Isolated
Story	RX(RS)	RX(RS)	RY(RS)	RY(RS)
	X(KN)	X(KN)	Y (KN)	Y (KN)
Roof	0	0	0	0
5F	220.79	92.66	220.52	93.33
4F	423.7	185.55	423.69	186.99
3F	593.27	272.9	593.15	275.4
2F	732.74	355.23	732.73	358.79
1F	843.75	433.25	843.66	437.9
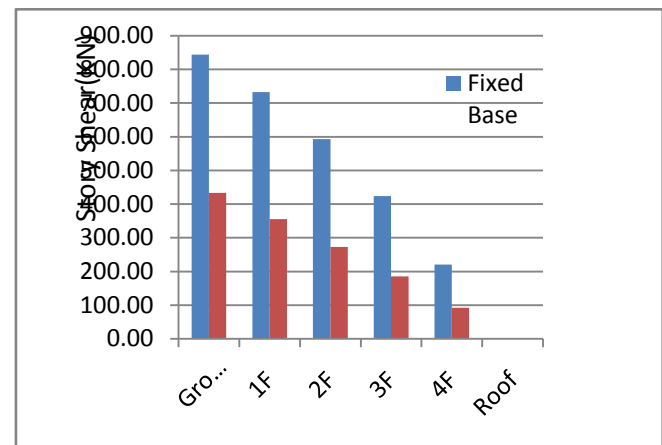
Figure-5 Story Shear vs Story Level

Table-4: Story Drift

	Fixed Base	Base Isolated	Fixed Base	Base isolated
Story	RX (RS)	RX (RS)	RY (RS)	RY (RS)
	Story	Story Drift	Story	Story Drift

	Drift (mm)	(mm)	Drift (mm)	(mm)
5F	1.351	0.7853	1.3506	0.6841
4F	2.177	1.2113	2.177	1.0823
3F	2.8773	1.6248	2.8771	1.4693
2F	3.427	2.0199	3.427	1.8419
1F	3.9144	2.7491	3.9142	2.5503

Table-5: Force & Moment in Beam

	Fixed Base			Base Isolated		
Beam No (93)	Left	Center	Right	Left	Center	Right
Shear Force (KN)	55.4	55.35	55.35	24	24	24
Moment (KNm)	96	12.93	70.09	43	7	29

Table-6: Force & moment in column

	Fixed Base		Base Isolated	
Column No (105)	Top	Bottom	Top	Bottom
Axial Force (KN)	121	121	47.6	48
Shear Force (KN)	36	36	15.3	15
Moment (KNm)	53.3	55.6	22.3	24

CONCLUSION

In this study it is quite clear that base isolation is quite effective in reducing the response as compared to fixed base system. Base isolation helps in reducing the design parameters i.e. bending moments in the structural members and base shear above the isolation by a considerable amount. The shear and the bending moments are reduced due to higher time period of the base isolated structure which results in lower acceleration acting on the structure due to base isolation devices. The absolute displacements increases but the relative displacements are reduced thus reducing the damages to the structure when subjected to an earthquake.

By the dynamic analysis it is seen that the base shear reduces by 50-55% in response spectrum analysis.

India is composed of strong, moderate and weak earthquake regions. Because of which consideration of vibration analysis in design is of great importance & interest. The seismic isolation analysis method has received the spotlight in many technologically advanced countries. With tremendously growing average lifestyle the interest for the safety aspect is also growing. Natural calamities are the most devastating among all the dangers, earthquake is one of the most dangerous natural calamity whose intensity can be predicted nor be combated when it hits. Hence engineers have to be equipped & prepared with the recent & modern safety systems in order to minimize the losses and damages.

REFERENCES

1. Lin A. N. (1992) "Seismic performance of fixed and Base isolated steel frames", Journal of Engineering. Mechanics, Vol.118, No. 5, pp. 921-941.

2. Kelly J.M. (1999)" the role of damping in seismic isolation Earthquake Engineering.Structure. Dynamic. 28, 320.

3. Jangid R.S. and Dutta T.K. (1995). "Seismic Behavior of Base-Isolated Buildings" Journal of Structural Engineering, 110: 186-203.

4. Hameed A., Thang D. and Jin-Hoon Jeong (2008). "Effect of Lead Rubber Bearing Characteristics on the Response of Seismic-isolated Bridges" KSCE Journal of Civil Engineering 12:187-196.

5. Jangid R.S. (1995). "Response of Pure-Friction Sliding Structure for Bi-Directional Harmonic Ground Motion", Journal of Structural Engineering, 19:97-104.

6. Jangid R.S. and Tongaonkar N.P. (2003). "Seismic response of isolated bridges with soil–structure interaction" Soil Dynamics and Earthquake Engineering 23, 287–302.

7. Eurocode-8, "Design of Structures for Earthquake Resistance", European Committee for Standardisation.

8. AASHTO. (1998). "Guide specifications for seismic isolation design." Washington, D.C.

9. Jangid R. S. (2004). "Seismic Response of Isolated Bridges" Journal of Bridge Engineering ASCE.

10. Chopra A.K. Ryan K.L. (2002) "Approximate analysis methods for asymmetric plan base-isolated buildings" Earthquake Engineering Structure. Dynamic. 31:33–54.

11. Chopra A.K. and Ryan K. L. (2004). "Estimating Seismic Demand on isolators in asymmetric building based on nonlinear analysis". Journal of earthquake engineering and Structural Dynamics.

12. Cardone D, Palermo G. Dolce M. (2010) "Direct Displacement-Based Design of

    Buildings with Different Seismic Isolation Systems" Journal of Earthquake Engineering, 14:163–191.

13. Chopra A.K. and Ryan K. L. (2004). "Estimating seismic displacement of friction pendulum isolators based on non-linear response history analysis." Journal of Earthquake Engineering and Structural Dynamics. 33:359–373.

14. Constantinou M.C. and Whittaker A.S. and Warn G.P. (2007). Performance of seismic isolation hardware under service and seismic loading, Technical report MCEER-07-0012.

15. Kelly S. E. (1986) "A seismic base isolation: review and bibliography", Soil Dynamic and Earthquake Engineering, Vol.5, No. 3, pp. 202-216.

16. Kelly, J.M., Naeim F. (1999) "Design of seismic isolated structures: From theory to practice" John Wiley and sons, Inc. New York.

17. Kulkarni J. A. and Jangid R.S. (2002). "Rigid body response of base isolated structures.

"Journal of structural control, 13:1230-1233.

18. Chopra, A. K. (2001). Dynamics of Structures Theory and Applications to Earthquake Engineering, second edition, Pearson Education publications.

    Deb S. K. (2004). "Seismic base isolation – An overview." Current science, 87:1426-1430.

● ● ●

Image Encryption By Using Visual Cryptography

[1]Madhavi Kale,[2]Prof.Nisha Lodha

[1]ME CSE Department of Computer Engineering G.H.Raisoni Institute,Jalgaon Maharashtra(MH), India

[2]Assi. Prof.Department of Computer Science EngineeringG.H.Raisoni Institute,Jalgaon Maharashtra(MH), India

Abstract- **Visual Cryptography is Data Security Technique which allows Visual Information like Picture, Text etc to be encrypted in a such way that decryption operation does not require Computer Visual Cryptography was introduced by Moni Naor and Adi ShamirThere are various Techniques to secure the images. There is One LZW data compression algorithm in that image is encrypted by using data compression but only .png and .gnf format is support.Visual Cryptography Scheme suffer from Transmission risk problem because the noise like shares will raise the suspicions of attackers and attacker might intercept the transmission There is one Halftone Visual cryptography which reduce transmission risk but faces some problems like Pixel expansion and Visual Quality Degradation. In proposed System Pixel Expansion and Visual quality Degradation these problems are solved by using combination of run length encoding algorithm and FOG removal algorithm. Also .jpeg format is supportable in LZW data Compression by using Huffman Coding Algorithm.**

Key words- **Visual Cryptography, Halftone, Pixel Expansion, visual Quality Degradation.**

I. INTRODUCTION

Visual Cryptography is a new Cryptography Technique which is used to secure the images. In Visual cryptography Image is divided into parts called Shares [1] and then they are distributed to the participants. the decryption side just stacking the share image gets the image. there is a secret image which is encrypted into some share images. The secret image is called the original secret image for clarity, and the share images are the encrypted images. When a qualified set of share images are stacked together properly, it gives a visual image which is almost the same as the original secret image or recovered secret image.

Visual Cryptography encrypts a secret image into shares such that stacking sufficient number of shares reveals the secret image. Shares are visually presented in transparencies. Visual Cryptography for Black and White was introduced by Moni Naor and Adi Shamir.[2] In Visual Cryptography for black and white image, one secret binary image is cryptographically encoded into n numbers of share of random binary pattern.[6] Share means Image is divided into parts is called Share. In the case of black and white images, the original secret image is represented as a pattern of black and white pixels. Each of these pixels is divided into sub pixels which themselves are encoded as black and white to produce the share images. and will focus on the black and white images, where a white pixel is denoted by the number 0 and a black pixels denoted by the number 1[4].

II. PREVIOUS WORK FOR VISUAL CRYPTOGRAPHY MODEL :

A. Visual Cryptography use for Secure the images

First Image is encrypt by dividing the original transparencies. And these transparencies can be sent to intended receiver. On the another Hand Transparencies received person can decrypt the transparencies using Tools and gets the original Image.

B. Visual cryptography for Binary Image

The original image is taken in the form of binary images, 1 for a black pixel and 0 for a white pixel. A single pixel from the original image is sub divided into two sub pixels in the share image
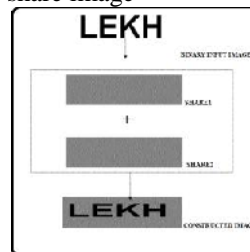

Figure 1: VCS for Binary Image

Visual Cryptography Schemes (VCS) is a method of image encryption used to hide the secret information in images.The secret image can be recovered simply by stacking the shares without any complex computation involved

C. Visual Cryptography for gray scale image

Transform the gray-level image into a black-and-white halftone image.

Figure 2:VCS for Gray scale Image

For each black or white pixel in the halftone image, decompose it into a 2×2 block of the two transparencies. If the pixel is white, randomly select one combination from the former two rows as the content of blocks in Shares 1 and 2. If the pixel is black, randomly select one combination from the latter two rows as the content of the blocks in the two transparencies

D. Visual cryptography for Color Model

Using the properties of the HVS to force the recognition of a secret message from overlapping shares, the secret image is decrypted without additional computations and any knowledge of cryptography. In Visual Cryptography for Color Model The additive and subtractive models are used[5].
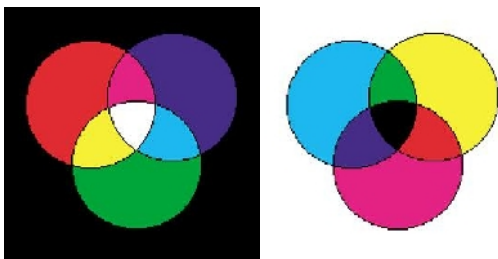

Figure 3:VCS for Color Image

Basic Principles of Color-

- Additive Model-primary Color (red blue and green) are mixed to obtain the desired color.[4] eg. Computer Screen.

- Subtractive Model-Color is represented by combinations of color lights reflected from the surface of an object.

III. PROBLEM STATEMENT:

Visual Cryptography scheme (VCs) generates random and meaningless share to share and protect secret images. Conventionally Visual Cryptography Scheme suffer from

Transmission risk problem because the noise like shares will raise the suspicions of attackers and attacker might intercept the transmission

Figure:4 (a) Original Image,(b) Proceed image after applying FOG removal algorithm

There is one halftone Visual Cryptography in that hiding Share Content in halftone share to reduce transmission risk. but Pixel Expansion and Visual Quality Degradation Problems are arise. Visual Cryptography Scheme (BVCS) reduce Transmission Risk and pixel Expansion problem reduce by RLE Compression Algorithm and Visual Quality Degradation Problem reduced by Combination of two Algorithm-RLE Compression algorithm and FOG Removal Algorithm.[7] A Technique for Image Encryption using LZW data Compression Algorithm, in that JPEG image does not Support. It suports only .png and .gnf format. To support JPEG format in LZW data compression Algorithm, Huffman encoding algorithm is use

IV. PROPOSED SOLUTION

To Solve Visual Quality degradation and Pixel Expansion Problem Run Length Encoding and FOG Removal Algorithm is Used. And also In LZW data Compression JPEG format is not Supportable. To Support JPEG Format in LZW data Compression we use Huffman Encoding Algorithm.

A. Run Length Encoding Algorithm:-

I. Procedure to compression of image by using RLE:

1. Read input image.
2. Separate image into component channel matrices
3. Run RLE on individual matrices
4. Use mono character symbols for replacement.
5. Use hybrid symbols
6. Append encoded matrices and dictionary to produce output.

II.Procedure to decompression of image by using RLE:

1. Read encrypted file information.
2. Separate dictionary and encrypted image information.
3. Create two temporary data references, one for mono character another for hybrid symbols

4. Match symbols in encrypted files with references 1& 2. If match found, retrieve the information and fill up the decrypted matrix for the corresponding channel.

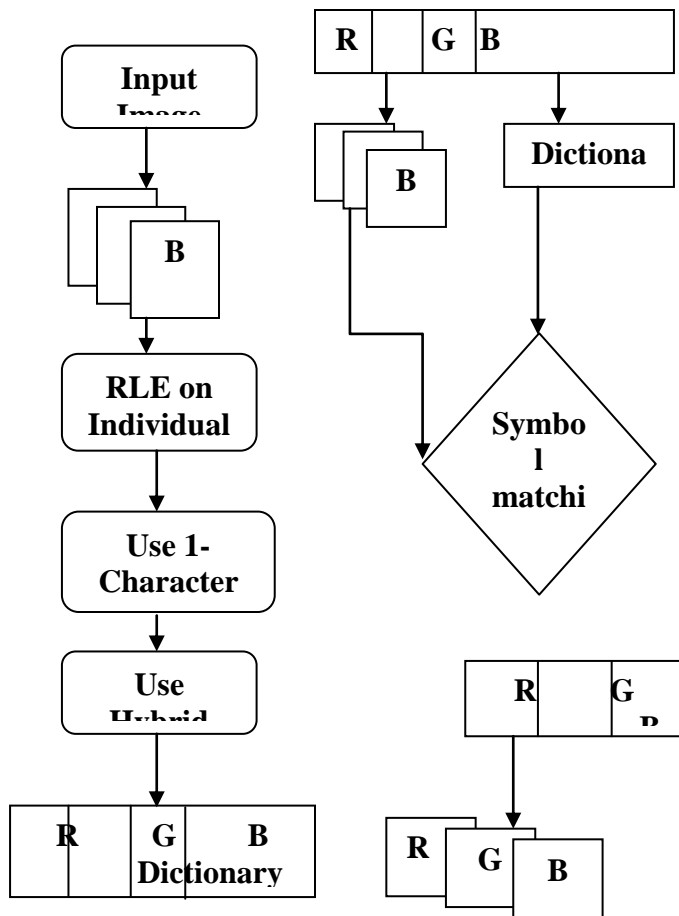5. Do the previous process for all channel matrices

The dark channel is defined to be the minimum over the entire patch of the minimum intensity over all three color channels.

Figure 5 (a)Run Length Enncoding compression Scheme (b)Run Length Encoding Decompression Scheme

B. FOG REMOVAL ALGORITHM:-

In the first step, the background depth map is calculated from two images, which are obtained from different weather condition. It is easy to get those images, because in outdoor surveillance applications, video cameras capture the same scene over long periods of time during which the weather may change. Also, the background depth map for the same scene only needs to be computed just once and not for every video frame. In the second step, we first calculate the observed depth map using the observed frame. Then the difference between the observed depth map and the background depth map is measured. Finally, the new object or the missing object in the current image will be extracted by the threshold method.

1. DARK CHANNEL PRIOR MODEL:

2. FOG PROPERTY MEASUREMENT:

dark channel prior only needs to be computed once for a fixed scene. Let Ic(M,N) denote the clear image, where M,N denote the image width and height, respectively.

3. ATMOSPHERIC   SCATTERING MODEL:-

poor visibility in bad weather is due to the substantial presence of atmospheric particles that have significant size and distribution in the participating transmission medium. Light from the atmosphere and light reflected from an object are absorbed and scattered by those particles, causing the visibility of a scene to be degraded.
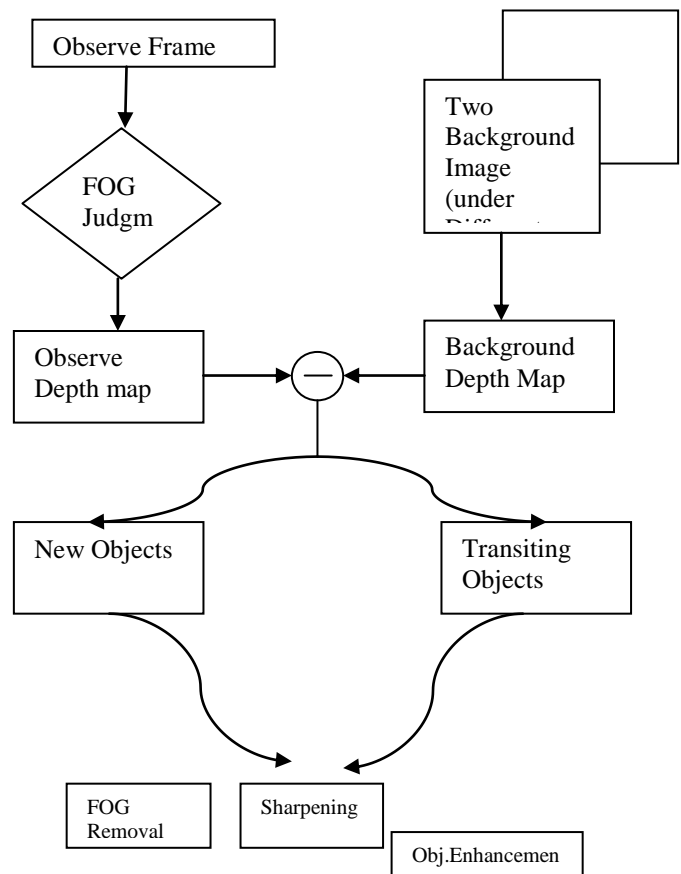

Figure 6: Procedure of FOG Removal Algorithm

V. DIRECT TRANSMISSION:

Because of the atmospheric scattering effect, a fraction of light flux is removed from the scene object.

VI. AIRLIGHT:

When direction transmission causes scene radiance to decrease with path length, airlight increases the light flux with path length. The airlight model describes a column of atmosphere acting as a light source by reflecting environmental illumination towards an observer.

VII. SHARPENING

Because the dark channel prior is calculated over each small patch, the transmission is constant in this patch, causing the restored image to contain some block effects. In order to smooth the restored image and preserve the object edges, the bilateral filtering algorithm isadopted to refine this image

C. HUFFMAN ENCODING ALGORITHM IN LZW DATA COMPRESSION TO SUPPORT JPEG FORMATHuffman coding is an entropy encoding algorithm used for lossless data compression[9]. The Huffman code refers to the use of a variable-length code table for encoding a source symbol (such as a character in a file) where the variable-length code table has been constructed in a particular way based on the estimated probability of occurrence for each possible value of the source symbol.[6]
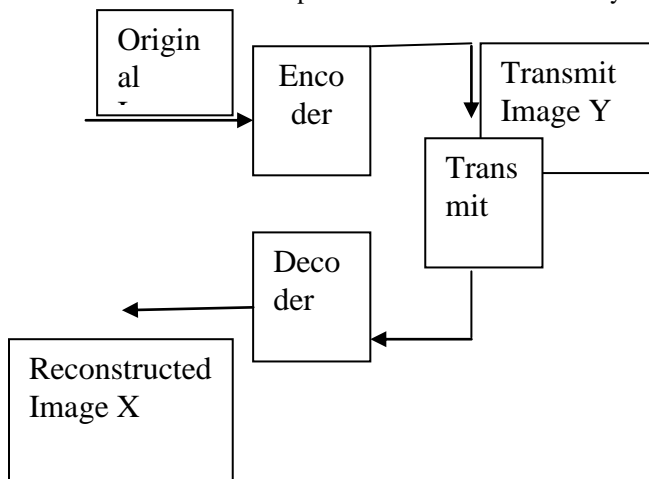

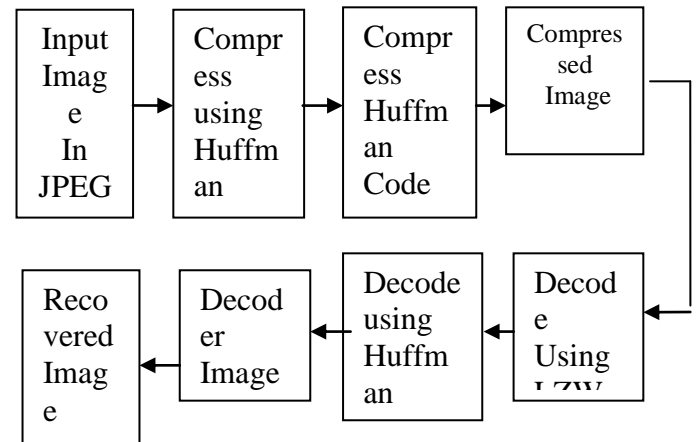Figure:7 Architecture of JPEG Image

Figure 8: Procedure of Huffman Encoding Algorithm

by using Huffman Encoding Algorithm

The decoding algorithm can re-create the same set of symbol frequencies from its de-compressed image pixels

CONCLUSION:-

In Visual Cryptography ,The decoded secret image quality is improve by using combination of two algorithm such as Run Length Encoding and FOG algorithm..

Visual Cryptography Scheme suffer from Transmission risk problem because the noise like shares will raise the suspicions of attackers and attacker might intercept the transmission There is one Halftone Visual cryptography which reduce transmission risk but faces some problems like Pixel expansion and Visual Quality Degradation. In Proposed System These two Problems are solved by RLE and FOG Removal algorithm.

There is one LZW data Compression algorithm in that, only .png and .gnf images are supportable to encrypt that image. In Proposed System .jpeg format is supportable by using Huffman Coding Algorithm in LZW data Compression. In Future we prove the Effectiveness and Flexibility of Image.

REFERENCES

[1] Xiang Wang , "A Lossless Tagged Visual Cryptography Scheme" IEEE Trans.on Signal Processing Letters and Security,VOL.21,NO.7,JULY 2014.

[2] Roberto De Prisco and Alfredo De santis, "On the Relation of random Grid and deterministic Visual Cryptography" IEEE Trans.on Information Forensic and Security,VOL.9,NO.4,APRIL 2014.

[3] Kai-Hui-Lee and Pei-Ling Chu, "Sharing Visual Secret in Single Image Random Dot Streogram" IEEE Trans.on Image Processing,VOL.23,NO.10,OCTOBER 2014.

[4] Velmurugan.N, Vijayaraj.A "Visual Pixel Expansion of Secret Image" Global Journal of Computer Science and Technology Volume 11 Issue 20 Version 1.0 December 2011.

[5] Sozan Abdulla," New Visual Cryptography Algorithm For Colored Image" JOURNAL OF COMPUTING, VOLUME 2, ISSUE 4, APRIL 2010, ISSN 2151-9617.

[6] Prakash Chandra Jena1, Nikunja Kanta Das2," A Survey on Visual Cryptography using Image Encryption and Decryption" International Journal of Emerging Technology and Advanced Engineering Certified Journal, Volume 3, Issue 8, August 2013.

[7] Manimurugan.S, Ramajayam.N ,"Visual Cryptography Based On Modified RLE Compression without Pixel Expansion "International Journal of Engineering and Innovative Technology (IJEIT) Volume 2, Issue 3, September 2012

[8] Gagandeep Singh1, Gagandeep Singh "EVALUATION OF VARIOUS DIGITAL IMAGE FOG REMOVAL ALGORITHMS" International Journal of Advanced Research in Computer and Communication Engineering Vol. 3, Issue 7, July 2014

[9] Aarti, Departmentof CSE,ACET India. Performance Analysis of Huffman Coding Algorithm" International Journal of Advanced Research in Computer Science and Software Engineering Volume 3, Issue 5, May 2013

[10] Maneesh Kumar1 and Sourav Mukhopadhyay2 "Visual Cryptography for Black and White Images" International Journal of Information and Computation Technology. ISSN 0974-2239 Volume 3,

● ● ●

Development of wavelet decomposition denoising algorithm for a linear FM chirp signal to apply any underwater communication systems.

[1]Venkataraman Padmaja,[2]Dr.V Rajendran
[1]Research Scholar, Satyabhama University,Chennai
[2] Professor, SSN college of Engineering, Chennai
[1]ktananya@gmail.com,[2]drvrajen@gmail.com

Abstract- **Underwater applications like Mine exploration, Pipeline / Cable laying, Hydrography, etc. warrant for different studies like Geo-technical, Geo-physical and other investigations in both Shallow and Deep water in the sea. Mostly, the mentioned studies are carried out using underwater marine acoustic instrumentations. The acoustic signals, in particular, shallow water suffers severe disturbances due to Ambient Noise in the sea. The Ambient noise in underwater is very unique, location specific and nearly deterministic also. Hence this paper aims at developing de-noising algorithm to improve the Signal to Noise Ratio (SNR) using the Uniform Filter Bank and Wavelet Packet Decomposition . The simulation was carried out using the MATLAB . The Ambient noise used for the validation is sea truth data collected in Bay of Bengal using the broad band Hydrophones. The results obtained was very encouraging as that in the range of input SNR -15dB to 0dB, the improved output SNR is order of 9dB. This shows the efficiency of algorithm simulated.**

Key words- **Underwater acoustic signal processing, underwater ambient noise, wavelet decomposition, underwater de-noising techniques.**

I. INTRODUCTION

Past two decades have seen advances in the research and development and deployment of underwater acoustic digital communication system. The area of primary interest is the military and deep sea research applications.[1].

In addition, un-tethered systems are also of increasing interest in a wide variety of applications, such as commercial fishing and oil exploration, where remotely controlled vehicles and equipment are used to probe, sense, and actuate apparatus from a surface vehicle or station. With increasing interest in environmental sensing, as well as continued exploration of the potential for research, commercial, and scientific applications in the oceans, the readily available of high-rate digital acoustic communications systems has become a catalyst for an explosion of applications. These applications range from command and control links to submarines and autonomous underwater vehicles and search-and-rescue contexts, to remote operation and control of sensing equipment in deep sea mining, off-shore oil exploration, and environmental monitoring[2]. Underwater acoustic signals are affected by shallow water condition and ambient noise during the transmission [3]. The shallow water ambient noises are both natural and human-made, with different sources exhibiting different directional and spectral characteristics. Therefore,

before recovering original signal from received acoustic signals, it is necessary to remove the present ambient noise so as to keep the important signal features as much as possible using matched filter concept[4] .

Wavelet packet decomposition[5] and the selection of the so–called "best basis"[6] in the sense of some criteria. It has been shown that an orthogonal wavelet basis is particularly adapted to discriminate signal and noise [7] the latter is represented by small coefficients on the wavelet domain. In that case, the "HardThresholding" [8] of the lowest coefficients leads to a noise reduction.

Gabor filter technique is projection of the signal into separate spectral channels and all filters have the same shape. In such space, the noise power is spread over all spectral channels and can be rejected by canceling all the coefficients below the noise threshold. As will be shown, the estimation of the noise threshold can be performed by means of high order statistics [9] [10] [11]

This paper aims at developing a de-noising algorithm to improve the Signal to Noise Ratio (SNR) using the most

match able Gabor Wavelet. The simulation was carried out using MATLAB. The Ambient noise used for the validation is sea truth data collected in Bay of Bengal using the broad band Hydrophones

II. CLASSIFICATION OF UNDERWATER NOISE

Acoustic noise can be considered as any sound other than the desired sounds. The ocean and many other bodies of water are very noisy with sounds being generated by the variety of different sources. The acoustic noise in the ocean is often referred to as ambient or background noise and is normally measured in terms of intensity in dB detected by an omni-directional hydrophone. Noise intensity may be measured in different frequency bands.

Ambient noise in shallow water tends to be highly variable, both in time and location. It is generally classified as given Fig 1. in the broad categories like wind , rain, ship, thermal based noises, etc.
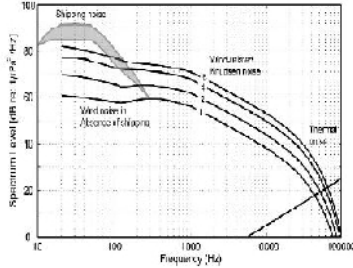

Fig.1. Classification of noise signal

III. DATA COLLECTION

For this particular work, Chennai has been selected in Bay of Bengal, as the data collection location. Generally, the data collection is done taking a reasonably equipped boat to a minimum of 30m depth shallow water and making a measurement.

Measurement system and its overview

The overall measurement arrangement which includes a boat in shallow water is given in Figure.2. In this arrangement the measurement system in particular consists of two hydrophones and its mounting arrangements, Data Acquisition System (DAS) and power supply. The calibrated omni directional hydrophone sensor with receiving sensitivity of -170dB with re 1V/μPa, over a frequency range 0.1 Hz to 25 kHz was used to measure the acoustic pressure of ambient noise. Both the hydrophones are mounted as shown in figure 3.5 in "L" shaped PVC tube filled with enough concrete so that it has got its self weight to sink in the underwater without floating or drifting due to shallow water environment. The other specifications of the measurement systems are provided in Table.1

Parameter	Specifications
Frequency of operation	Upto 25kHz
Directivity	Omni directional
Sensitivity	-170dB
Type of material	Piezo electric (PZT)
Operating depth	600 m
Survival depth	700 m
Operating Temperature range	-2 to +55 C
Operating Voltage	12 to 24 VDC

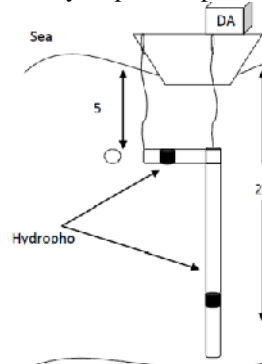Table 1: Hydrophone Specifications

Fig 2.Measuring arrangement in the sea

IV. SIGNAL DENOISING TECHNIQUES

Underwater de-noising techniques are classically based on the projection of the ambient noisy signal on a new space[12], in which the signal and the noise do not overlap. The ambient noise in view of new space projection is eliminated by preserving the signal into subspace only. Applying into inverse projection technique, a denoised form of the original signal is recovered.

In view of applying projection techniques, is the class of unitary transforms since they have the more useful properties for underwater signal processing. Among all, unitary transforms assure that the existence of an inverse transform technique and preserve the acoustic signal energy on the transformed space. Fig3. Wenz model [12] of the power spectral density of the underwater ambient noise.

The underwater denoising techniques considered here are based on this framework: the acoustic signal is projected on a new space with a unitary transform technique, properly filtered in this new space and, with the inverse unitary transform technique, estimated back to the original signal space.
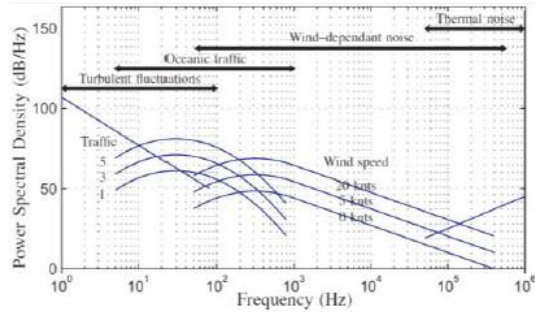
Fig.3 Wenz model [12] of the power spectral density of the underwater ambient noise

Wavelet Packet Decomposition

Wavelet has generated a tremendous interest in both applied and theoretical areas [13],[14]. The wavelet transform theory provides an alternative tool for short time analysis of quasi stationary signal such as Speech as opposed to traditional transforms like FFT. Wavelet analysis is a powerful and popular tool for the analysis of non-stationary signals. The wavelet transform is a joint function of a time series of interest d(t) and an analyzing function or wavelet. This transform isolates signal variability both in time t, and also in "scale" s, by rescaling and shifting the analyzing wavelet.

Wavelet packet decomposition (WPD) is extended from the wavelet decomposition (WD). It includes multiple bases and different basis will result in different classification performance and cover the shortage of fixed time–frequency decomposition in DWT. The algorithm of the wavelet packet decomposition and reconstruction is

$$u^{j}_{2m}(n) = \sum_k h(k - 2n) u^{j-1}_m(k) \qquad (1)$$

$$u^{j}_{2m+1}(n) = \sum_k g(k - 2n) u^{j-1}_m(k) \qquad (2)$$

$$u^{j-1}_m(n) = \sum_k H(k - 2n) u^{j}_{2m}(k) + \sum_k G(k - 2n) u^{j}_{2m+1}(k) \qquad (3)$$

Determination of threshold function

On wavelet packet de-noising, threshold function is embodied that it adopts different strategy to deal with coefficients accordingly which is more or less than the threshold. Soft and hard threshold function has been widely applied.

$$\hat{w}_{j,k} = \begin{cases} Wj,k, & |Wj,k| \geq \lambda \\ 0 & |Wj,k| < \lambda \end{cases} \qquad (4)$$

$$\hat{w}_{j,k} = \begin{cases} sgn(Wj,k)(|Wj,k| - \lambda), & |Wj,k| \geq \lambda \\ 0 & |Wj,k| < \lambda \end{cases} \qquad (5)$$

Where

sgn = sign function

λ – threshold ,

W = represents wavelet coefficients of signal decomposition,

$\hat{w}$ Estimated value of wavelet coefficients by thresholding.

A Gabor filter expressed by

$$h_{b_i}(t) = \frac{1}{\sigma_i \sqrt{2\pi}} \exp\left(\frac{-t^2}{2\sigma_i^2}\right) \exp(j2\pi b) \qquad (6)$$

σ_i^2 Variance of Gaussian envelope signal

b_i Frequency of the complex harmonic signal and the sample wavelet
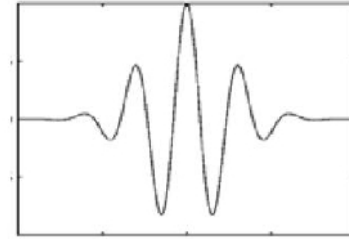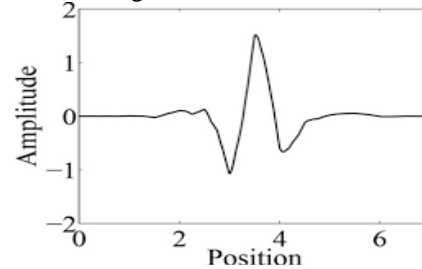

Fig.4.Gabor Wavelet

Fig 5. Symlet wavelet

For comparative purpose, Symlet filter is also taken for the study. The symlets are nearly symmetrical, orthogonal and biorthogonal wavelets proposed by Daubechies as modifications to the db family. The properties of the two wavelet families are similar. Wavelet is shown in figure 5.

Let assume a frequency bandwidth of interest area $[b_{min} ; b_{max}]$ which will cover the different filter frequency range. Gabor filter with frequency equal to the centre of the sub-band. The representation of any bandwidth signal d(t)

$$\in L^2(\mathbb{R}) d_{b_i}(t) = h_{b_i}(t) * d(t), b_i \in [b_{min} ; b_{max}], i = 1, \ldots \ldots \quad (7)$$

The transformation is unitary if

$$\mathcal{F}[h_{b_1}(t) + \cdots + h_{b_N}(t)](b) = 1, b, b_i \in [b_{min} ; b_{max} \quad (8)$$

Where

$\mathcal{F}[d(t)](b)$ Fourier transform of the signal d(t)

$\Gamma[x(t)](v)$ denotes the fourier transform of the signal x(t)

This condition implies that the number of filters and of the Gaussian envelope signal have to be carefully chosen to verify (8). If this condition is satisfied, the inverse unitary operator has a simple as it is the sum of all spectral channels. The Gabor filter provides the Time-Frequency representation of the given signal.

For a noisy coherence signal, the each spectral channel has various statistical properties. In overview, coherent components are characterized, in the Time-Frequency plane, by high and concentrated coefficients while noise is characterized by low and spread coefficients. Therefore, noise reduction has done by using thresholding lowest coefficients leads. The estimation of the noise threshold can be addressed with higher–order–statistics [5]. The root–mean–square (RMS) expressed by

$$E_\sigma(t) = \sqrt{\frac{1}{N}\sum_i d_{b_i}^2} \qquad (9)$$

This expressed equation gives the mean energy value at a specific time and over each spectral channel. At a time when only the ambient noise is present, the quantity of energy value over the spectral channels is the energy value of the ambient noise. By contrast, at a time when noise and signal are both present, the quantity of energy value over the spectral channels is the energy value of the signal and the energy value of the ambient noise. The result shows that, the RMS value is low when noise only present and high if signal and noise are both present. In the later section, Fig.10 shows the Gabor filter response for various sigma values.

SIMULATION AND EXPERIMENT

A gated linear FM wave as signal (acoustic) e(t) is assumed to be transmitted through a mid frequency water channel and the simulated signal is given in Fig.6
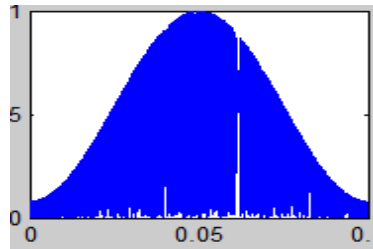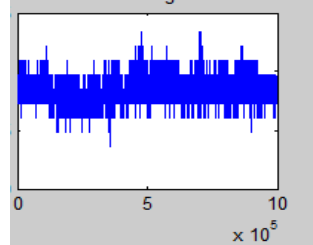

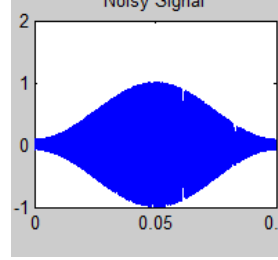Fig.6 Gated Linear FM signal

Fig.8 Noise signal

Fig.9 Noisy Signal

For analyzing the signal is added with the underwater ambient noise which collected in Chennai, at Bay of Bengal given in Fig.8. The reference signal is simulated at 20kHz. The noise data is the real time data collected and is assumed to be stationary, gaussian, with a Wenz–shaped power spectral density (Fig.3). The results have been obtained with 50 different noise realizations and have to be taken in an average.

The proposed de-noising methods reduce the noise while preserving the useful part of the signal. Each method has different type of performance with regards to the recovery of the signal boundary. Fig. 10 shows the Schematic representation of the simulation procedure.

Fig.11 shows, as one example, the Gabor filter response for various sigma values. . These results come from the non–linearity of the Hard Threshold procedure, which suppress a few wavelet coefficients that are involved in less noise reduction performance. By selecting the number of retained principal components using Kaiser's rule, the noise removal is done and its shows that better performance higher sigma value although there is considerable reduction in the signal level. It is visually more satisfactory by seeing the time series original signal. It gives the best results and better performance
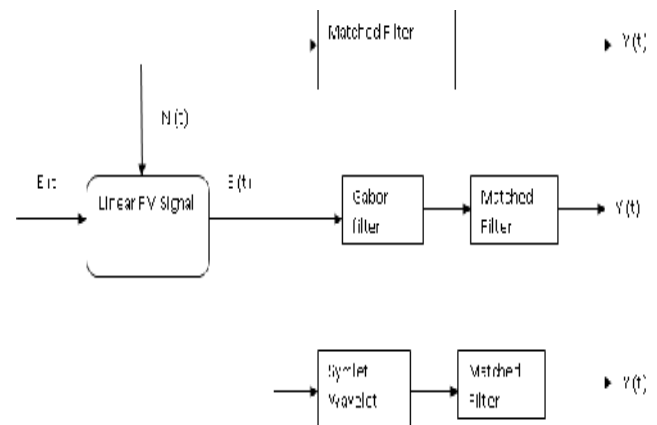

Fig.10 Schematic representation of the simulation procedure

Fig.12 shows input signal–to–noise ratio (input SNR) versus the output signal–to–noise ratio (output SNR) and used expressions are

$$SNRIn = 10 * Log_{10} \frac{Input\ power}{Noise\ power}\ (dB) \qquad (10)$$

$$SNROut = 10 * Log_{10} \frac{Output\ power}{Noise\ power}\ (dB) \qquad (11)$$

Where "Input power" and "Output Power" are respectively the signal power before and after denoising, and "Noise power" are respectively on the same frequency band of the signal. From the Fig 12 , it is revealed that all three methods lead to an improvement of the SNR in which confirm a significant reduction of the noise. However, this suggests that only Gabor filter gives the improved output SNR is order of 9dB in the range of input SNR -15dB to 0dB. This shows the efficiency of algorithm simulated.
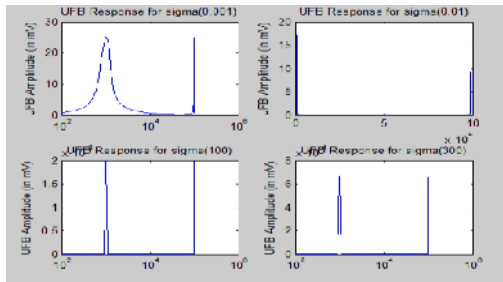

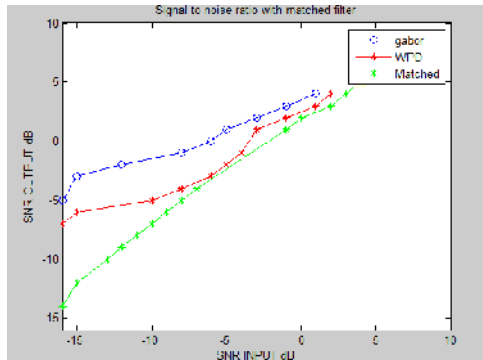Fig.11.Gabor filter response for different sigma values

Fig.12 Comparative analysis of the de-noising procedures to improve SNR.

CONCLUSION

In this paper, it is explained that underwater acoustic instruments plays prominent role in exploration and exploitation of both living and non-living ocean resources of many varieties of underwater applications. It is observed that the acoustic signals, in particular, shallow water suffers severe disturbances due to Ambient Noise in the sea. The Ambient noise in underwater is very unique, location specific and nearly deterministic also. It is important that the development of de-noising algorithm with an appropriate technique. In addition, validating the mentioned algorithm with sea-truth ambient noise collected at particular location is also equally important. So, the noise in underwater is collected in Chennai at Bay of Bengal and it is found that the collected noise is a composite of various sources with miscellaneous spectral characteristics. To overcome this primal limitation, the most proven de-noising techniques, wavelet decomposition with two different wavelet (Gabor and Symlet) have been studied. This technique is based on the transformation of the signal on a unitary space. This assurance the existences of an inverse transform.

On this new space, a FIR filtering method has been applied to remove the noise. Finally, performances of the two de-noising technique procedures with two different wavelets (Gabor and Symlet) have been investigated with realistic simulated data. Results show that these methods lead to a noise reduction. However, the proposed Gabor filter–based denoising method gives better results. It leads to a better noise reduction and significant improvement. The results obtained was very encouraging as that in the range of input SNR -15dB to 0dB, the improved output SNR is order of 9dB. This shows the efficiency of algorithm simulated. Future works concern a firmware implementation of a new class of Time Frequency filters adapted to underwater environment signals whose frequency content varies strongly in time.

REFERENCES

[1] M.Ravindran, and V.Rajendran. 1999. Indigenous Marine Acoustic Instruments. Journal of Acoustical Society of India XXVII : 57-62
[2] Andrew C. Singer, Jill K. Nelson, and Suleyman S. Kozat, "Signal Processing for Underwater Acoustic Communications," UNDERWATER WIRELESS COMMUNICATIONS, IEEE Communications Magazine ,January 2009.
[3] E.Westwood and C. Tindle, "Shallow water time–series simulation using ray theory," Journal of the Acoustical Society of America, vol. 81, June 1986.
[4] M. Stojanovic, "Underwater acoustic communications," in Encyclopedia of Electrical and Electronics Engineering, vol. 22, pp. 688–698, John G. Webster, John Wiley & Sons, 1999.
[5] GUO Jiyun, WANG Fuming., "Signal De-noising Based on Wavelet Packets Transform", Journal of Modern Electronics Technique, 2007, (19): 55-56.
[6] S. Mallat, A wavelet tour of signal processing. Academic Press, 1998.
[7] D. Donoho and J. I.M., "Adapting to unknow smoothness via wavelet shrinkage," Journal of American Statistical Association, vol. 90, pp. 1200–1224, Dec. 1995.
[8] H. Krim, D. Tucker, S. Mallat, and D. Donoho, "On denoising and best signal representation," IEEE Trans. on Information Theory, vol. 45, pp. 2225–2238, Nov. 1999.
[9] P. Ravier and P. Amblard, "Wavelet packets and de-noising based on higher-order statistics for transient detection," Signal Processing, vol. 81,Aug. 2001.
[10] P. Moreno, A. Bernardino, and J. Santos-Victor, "Gabor parameter selection for local feature detection," IBPRIA - 2nd iberian Conference on Patterns Recognition and Image Analysis, Estoril,Portugal, June 2005.

[11] A. K. Jain, N. K. Ratha, and S. Lakshmanan, "Object detection using Gabor filters," Pattern Recognition, vol. 30, pp. 295–309, 1997.

[12] G. Wenz, "Review of underwater acoustics research: Noise," Journal of the Acoustical Society of America, vol. 34, pp. 1936–1956, Dec. 1962.

[13] Seok, J. W. "Speech enhancement with reduction of noise components in the wavelet domain", International conference on audio, speech and signal processing of IEEE, 1997.

[14] J.Z. Xue, H. Zhang, C.X. Zheng," Wavelet packet transform for feature extraction of EEG during mental tasks", Presented at Proceedings of the Second International Conference on Machine Learning and Cybernetics, Xi'an, 2003.

●　●　●

Improving the Security of Caesar Cipher Using Row Shift and Column Transformation

[1]Ahmad Rufa'i, [2]A.A Ibrahim,[3]Zaid Ibrahim,[4]Saidu Yakubu

[1][2][3]Sokoto State University, [4] College of Nursing and midwifery, Sokoto

[1]rufaiahmad35@yahoo.com ,[2] aminuibrahim40@gmail.com,[3] malamzaid2@yahoo.com,[4] saiyad27@yahoo.com

Abstract- **Data security has become a very important aspect in recent years due to drastic progress in the use of internet. Many ciphers have been developed to provide data security but all the conventional encryption techniques have proved to be weak and amenable to attack even by use of brute force and traditional cryptanalysis. Caesar cipher is the simplest and weakest because it can be simply attacked by brute force cryptanalysis. This work proposes an improvement over Caesar cipher by using row shift and column transformations. The improvement will no doubt eliminate the weakness of the Caesar cipher and provide ciphertext that is harder to crack.**

Key words- **Caesar cipher, Brute force attack, Row Shifting, Column Transformation, Self inverse.**

I. INTRODUCTION

In recent time, the internet has positioned itself to providing essential communication between millions of people and is being increasingly used as a tool for paperless transaction in business, private or governmental offices by means of e-mail messages, e-cash transactions and so on. Due to this development there is a great need for transmission of data through internet in various businesses, private and governmental sectors. Part of this information is sensitive and confidential like banking transactions, credit information, governmental information and so on. Moreover, sensitive information is transferred over web using e-mails and so on.

The confidentiality, authentication and integrity of such important information need to be maintained and protected. To protect this type of sensitive information from an unauthorized access, experts have come up with solutions embodied in the concept of 'cryptography'. Cryptography is the study of sending and receiving secret messages. The aim of cryptography is to send messages across a channel so that only the intended recipient of the message can read it. In addition, when a message is received, the recipient usually requires some assurance that the message is authentic; that is, that it has not been sent by someone who is trying to deceive the recipient. The message to be sent is called the plaintext message. The disguised message is called the ciphertext. The plaintext and the ciphertext are both written in an alphabet, consisting of letters or characters. Characters can include not only the familiar alphabetic characters A,…,Z and a,…, z but also digits, punctuation marks, and blanks. A cryptosystem, or cipher, has two parts: encryption,

the process of transforming a plaintext message to a ciphertext message, and decryption, the reverse transformation of changing a ciphertext message into a plaintext message [1]. Caesar cipher is one of the most widely known encryption and decryption cipher. It is also the simplest and weakest cipher [2].

The process of encryption and decryption of data is shown below:
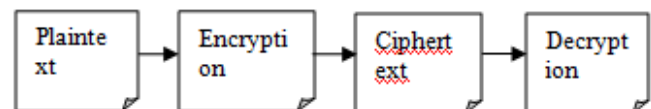
Fig.1.1.1. Encryption and Decryption [5].

By using cryptography many goals can be achieved. These goals can be either all achievable in some applications at the same time or only one of them being achieved. The goals of cryptography include:

(i) Confidentiality: this is the most important goal which ensures that nobody can understand the received message except the one who has the deciphering key.

(ii) Authentication: this is the process of providing the identity that assures communicating entity is the one that it claimed to be, which applies to both entities and information itself.

(iii) Data Integrity: this is a service which addresses the unauthorized alteration of data

(iv) Non-Repudiation: it is a mechanism used to prove that the sender really sent message and message was received by the specified party, so the recipient cannot claim the message was not sent.

(v) Access control: it is the process of preventing an unauthorized use of resources. This goal controls who can access the resources [6].

II. REVIEW OF THE LITERATURE

The earliest form of cryptography was the simple writing of a message that cannot be read by other people. In fact, the word 'cryptography' comes from two Greek words 'cryptos' and 'graphein' which means hidden and writing respectively. The need to conceal message has been with us since we move out of caves, started living in groups and decided to take this civilization idea seriously [1]. The Greek's idea was to wrap a tape around a stick and then write the message on the wound tape. When the tape was unwounded the writing would be meaningless. The receiver of the message would of course have a stick of the same diameter and use it to decipher message [5].

The Roman method of cryptography was known as Caesar cipher, named after Julius Caeser who apparently used it to communicate with his generals. It is one of the earliest known and simplest ciphers. The Caesar cipher involves replacing each letter of the alphabet with the letter standing three places further down the alphabet. For example,

Plaintext: MEET ME AFTER THE TOGA PARTY
Ciphertext:PHHW PH DIWHU WKH WRJD SDUWB

If it is known that a given ciphertext is a Caesar cipher, then a brute-force cryptanalysis is easily performed: simply try all the 25 possible keys. Figure below shows the results of applying this strategy to the example ciphertext. In this case, the plaintext leaps out as occupying the third line [5].

KEY
1   OGGV OG CHVGT VJG VQIC RCTVA
2   NFFU NF BGUFS UIF UPHB QBSUZ
3   MEET ME AFTER THE TOGA PARTY
4   LDDS LD ZESDQ SGD SNFZ OZQSX

Many ciphers have been developed to protect the confidential information, but almost all the conventional ciphers are proved to be weak and amenable to attack even by the use of brute force and traditional cryptanalysis. Hence there is a need to develop stronger and more secure ciphers that will overcome the shortcomings and weaknesses of the conventional ciphers, either by modification, combination and so on.

III. PROPOSED WORK

In this work Caesar cipher will be combined with row shift, column transformation and additional key.

A. Row shift
This involves shifting the rows of the grid from right to left the first row does not shift at all.

B. Column transformation
In column transformation we take each column separately and replace it with one where each entry is the sum of all other entries in the column. The addition is exclusive OR after turning each letter to binary digits.

C. Encryption algorithm
Step I: Encrypt the plaintext using the Caesar cipher.
Step II: Write the encrypted message as $m \times m$ grid (top to bottom and left to right).
Step III: Shift the rows of the grid (R-L) using shift of nth row $= (n-1)$ shift.
Step IV: add secret Key(s).
Step V: Transform each column.

D. Decryption algorithm
Step I: Read the ciphertext and write as $m \times m$ grid (top to bottom and left to right).
Step II: Transform each Column.
Step III: add Secret key(s).
Step IV: Shift the rows of the grid (L-R) using shift of nth row $= (n-1)$ shift.
Step V: Write all the component of the matrix in a straight line (from top to bottom and left to right), and decrypt using Caesar cipher

IV. ENCRYPTION AND DECRYPTION USING PROPOSED SYSTEM

Correspondence Table (character – binary number)

Character	Binary
η	00000
A	00001
B	00010
C	00011

D	00100
E	00101
F	00110
G	00111
H	01000
I	01001
J	01010
K	01011
L	01100
M	01101
N	01110
O	01111
P	10000
Q	10001
R	10010
S	10011
T	10100
U	10101
V	10110
W	10111
X	11000
Y	11001
Z	11010
Space(_)	11011
!	11100
.	11101
,	11110
?	11111

$$!+C = +\frac{11100}{00011}$$

$$W + O = +\frac{10111}{01111}$$
$$\overline{11111} = ?$$

$$11000 = X$$

$$U + N = +\frac{10101}{01110}$$

$$C + F = +\frac{00011}{00101}$$

$$11011 = \quad \_$$

00101= E
Continuing in this way we get
L + E = I

$$N + R = !$$

η + E = E

$$, + N = P$$

R + C = Q

$$\eta + E = E$$

V + _ = M

$$Z + X = B$$

, + X = F

$$H + ! = T$$

, + ! = B

$$V + ! = J$$

Thus,

$$\begin{pmatrix} ? & I & Q & F \\ X & ! & E & T \\ \_ & E & M & B \\ E & P & B & J \end{pmatrix}$$

A. Encryption

Suppose we want to encrypt "YES IT WORKS !!" using keys CONFERENCE XX!!! and TRANSFORMATIONXY

!HV,LW,ZRUNV

$$\begin{pmatrix} ! & L & R & , \\ H & W & N & \eta \\ V & , & U & \eta \\ , & Z & V & C \end{pmatrix} \Rightarrow \begin{pmatrix} ! & L & R & , \\ W & N & \eta & H \\ U & \eta & V & , \\ C, & , & Z & V \end{pmatrix}$$

$$\Rightarrow \begin{pmatrix} ! & L & R & , \\ H & W & N & \eta \\ V & , & U & \eta \\ , & Z & V & C \end{pmatrix} + \begin{pmatrix} C & E & C & X \\ O & R & E & ! \\ N & E & \_ & ! \\ F & N & X & ! \end{pmatrix}$$

Similarly, adding the second key we have

$$\begin{pmatrix} ? & I & Q & F \\ X & ! & E & T \\ \_ & E & M & B \\ E & P & B & J \end{pmatrix} + \begin{pmatrix} T & S & M & O \\ R & F & A & N \\ A & O & T & X \\ N & R & I & Y \end{pmatrix}$$

? + T = K

$$X + R = J$$

_ + A = Z

$$E + N = K$$

I + S = Z

$$! + F = Z$$

E + O = J

$$P + R = B$$

Q + M = !

$$E + A = D$$

M+ T = Y

$$B + I = K$$

F + O = I

$$T + N = Z$$

B + X = Z

$$J + Y = S$$

Thus, $\begin{pmatrix} K & Z & ! & I \\ J & Z & D & Z \\ Z & J & Y & Z \\ K & B & K & S \end{pmatrix}$

Column transformation

$$\begin{pmatrix} K \\ J \\ Z \\ K \end{pmatrix} \Rightarrow \begin{pmatrix} J + Z + K \\ Z + K + K \\ K + K + J \\ K + J + Z \end{pmatrix} \Rightarrow \begin{pmatrix} \_ \\ Z \\ J \\ \_ \end{pmatrix}$$

$$\Rightarrow \begin{array}{r} 01010 \\ +11010 \\ \hline 01011 \end{array}$$

$$\begin{array}{r} 11010 \\ +01011 \\ \hline 01011 \end{array}$$

$$11011 = \_$$
$$11010 = Z$$

$$\begin{array}{r} 01011 \\ +01011 \\ \hline 01010 \end{array}$$

$$\begin{array}{r} 01011 \\ +01010 \\ \hline 11010 \end{array}$$

$$01010 = J$$
$$11011 = \_$$

For the second column

$$\begin{pmatrix} Z \\ Z \\ J \\ B \end{pmatrix} \Rightarrow \begin{pmatrix} R \\ R \\ B \\ J \end{pmatrix}$$

For the third column

$$\begin{pmatrix} ! \\ D \\ Y \\ Z \end{pmatrix} \Rightarrow \begin{pmatrix} V \\ N \\ S \\ A \end{pmatrix}$$

For the last column

$$\begin{pmatrix} I \\ Z \\ Z \\ S \end{pmatrix} \Rightarrow \begin{pmatrix} S \\ \eta \\ \eta \\ I \end{pmatrix}$$

Thus, $\begin{pmatrix} \_ & R & V & S \\ Z & R & N & \eta \\ J & B & S & \eta \\ \_ & J & A & I \end{pmatrix}$

Which gives our ciphertext as: _ZJ_RRBJVNSAS $\eta\eta I$

   A. *Decryption*

_ZJ_RRBJVNSAS $\eta\eta I$

$$\begin{pmatrix} \_ & R & V & S \\ Z & R & N & \eta \\ J & B & S & \eta \\ \_ & J & A & I \end{pmatrix}$$

Now, for column transformation we have,

$$\begin{pmatrix} \_ \\ Z \\ J \\ \_ \end{pmatrix} \Rightarrow \begin{pmatrix} Z + J + \_ \\ J + \_ + \_ \\ \_ + \_ + Z \\ \_ + Z + J \end{pmatrix} \Rightarrow \begin{pmatrix} K \\ J \\ Z \\ K \end{pmatrix}$$

Because, $\begin{array}{r} 11010 \\ +01010 \\ \hline 11011 \end{array}$

$$\begin{array}{r} 01010 \\ +11011 \\ \hline 11011 \end{array}$$
$$01011 = K$$

$$01010 = J$$

11011

+11011

11010

11011

+11010

01010

11010 = Z

01011 = K

Continuing this way we have,
Second column:

$$\begin{pmatrix} R \\ R \\ B \\ T \end{pmatrix} \Rightarrow \begin{pmatrix} Z \\ Z \\ J \\ R \end{pmatrix}$$

Third column:

$$\begin{pmatrix} V \\ N \\ S \\ A \end{pmatrix} \Rightarrow \begin{pmatrix} ! \\ D \\ Y \\ K \end{pmatrix}$$

Fourth column:

$$\begin{pmatrix} S \\ \eta \\ \eta \\ I \end{pmatrix} \Rightarrow \begin{pmatrix} I \\ Z \\ Z \\ S \end{pmatrix}$$

$$\Rightarrow \begin{pmatrix} K & Z & ! & I \\ J & Z & D & Z \\ Z & J & Y & Z \\ K & B & K & S \end{pmatrix}$$

Adding with the second key we have,

$$\begin{pmatrix} K & Z & ! & I \\ J & Z & D & Z \\ Z & J & Y & Z \\ K & B & K & S \end{pmatrix} + \begin{pmatrix} T & S & M & O \\ R & F & A & N \\ A & O & T & X \\ N & R & I & Y \end{pmatrix}$$

K + T = ?

J + R = X

Z + A = _
Z + S = I
J + O = E
! + M = Q
= E

K + N = E
Z + F = !
B + R = P
D + A

Y + T = M
= B
I + O = F
= T
Z + X = B
= J

K + I

Z + N

S + Y

Adding with the first key we have,

$$\begin{pmatrix} ? & I & Q & F \\ X & ! & E & T \\ \_ & E & M & B \\ E & P & B & J \end{pmatrix} + \begin{pmatrix} C & E & C & X \\ O & R & E & ! \\ N & E & \_ & ! \\ F & N & X & ! \end{pmatrix}$$

$\Rightarrow$? + C = !
X + O = W
_ + N = U
E + F = P
I + E = L
! + R = N
E + E = η
P + N = ,
Q + C = R
E + E = η
M + _ = V
B + X = Z
F + X = ,
T + ! = H
B + ! = ,
J + ! = V

Thus, $\begin{pmatrix} ! & L & R & , \\ W & N & \eta & H \\ U & \eta & V & , \\ C, & , & Z & V \end{pmatrix}$

We now shift the rows (R – L) using shift of nth row = $(n-1)$ shift.

$$\begin{pmatrix} ! & L & R & , \\ H & W & N & \eta \\ V & , & U & \eta \\ , & Z & V & C \end{pmatrix}$$

Decrypting using Caesar cipher we have,

YES IT WORKS !!

Hence, the original text.

CONCLUSION

The improved method is a combination of Caesar cipher with row shift, column transformation and additional key(s)

that provides secured and strong cipher. The improved system resulting from the merger of Caesar cipher, row shift, column transformation and addition of additional key(s) is becoming more complicated than some algorithms operated to work independently. The advantage of the system is that, it provides better security because even if some component ciphers are broken or some of the secret keys are recognized, the confidentiality of the original data can still be maintained.

REFERENCES

[1] Judson, W.T., (2010). Abstract Algebra Theory and Aplications, Austin State University, P. 100 – 101.

[2] Goyal, K. and Kinger, S. (2013). Modified Caesar cipher for better security enhancement, International Jouranal of Computer Application, 3, 28-29.

[3] Ajit, S., Nandal, A. and Malik, S. (2012). Implementation of Caesar cipher with Rail Fence for Enhancing Data security. International Journal of Advanced Research in Computer Software Engineering, 2(12), 78-80.

[4] Srikantaswamy, S.G. and Phaneendra, H.D. (2012). Improved Caesar Cipher with Random Number Generation Technique and Multistage Encryption. International Journal on Cryptography and Information Security (IJCIS), 2(4), 40-46.

[5] Stallings, W. Cryptography and Network security, principles and practice. Fifth edition, Prentice Hall, New York, pp. 243-323.

[6] AbuTaha, M., Farajallah, R.T. and Mohammed, O. (2011). Survey Paper: Cryptography is TheScience of Information Security. International Journal of Computer Science and Security, 5(3), 298-304.

● ● ●

Mining YouTube Videos Metadata
for Cyberbullying Detection

[1]Mr. Shivraj Sunil Marathe, [2]Prof. Kavita P. Shirsat
[1]M. E. Student,[2]Assistant Professor
Vidyalankar Institute of Technology, Wadala (E), Mumbai, India
[1]shivraj.marathe@vit.edu.in, [2]kavita.shirsat@vit.edu.in

Abstract- **Recent years have witnessed the evolution of Web 2.0, which has drastically increased the volume of community-shared textual resources (posts, comments) and media resources (videos, images) over the web. Moreover, today the internet has become an effective communication platform for people. Because of which many cyberbullying content promoters have also been attracted towards online social networks. Online video sharing websites such as YouTube contain large number of videos and users promoting cyberbullying and harassment. Due to immense popularity, anonymity and fewer restrictions for publication, YouTube is misused by some users to promote cyberbullying and online harassment.**

Our research presents an approach to identify misdemeanor, harassment resulting in cyberbullying by mining the video metadata. We conduct a study on a training dataset obtained by extracting several videos metadata using YouTube API. We formulate the problem of identifying cyberbullying videos as a search problem and present Shark Search algorithm based approach for cyberbullying detection. We present the result using standard information retrieval metrics such as f-measure, precision and recall. The accuracy of the proposed solution on the sample dataset is 83.65%. Our result favors the requirement of several contextual meta-data like, terms present in the title of the videos, description and comments, video subscribers and likes, number of views, YouTube category, length of videos and content focus in cyberbullying detection.

Key words- **Cyberbullying, Information Retrieval, Mining User Generated Content, Online Harassment Detection, Text Mining, YouTube, Video Sharing Sites**

I.   INTRODUCTION & MOTIVATION

With the proliferation of the Internet, online security of an individual has become an important concern. While Web 2.0 provides easy, interactive, anytime and anywhere access to the online communities, it also provides an avenue for cybercrimes like cyberbullying.

Now-a-days, online social networking websites such as Facebook, Twitter, YouTube, Instagram, Flickr etc. are experiencing a huge growth in popularity. In particular, video content is becoming a most important part of user's daily life. By allowing users to generate and distribute their own multimedia content to public, the Web has transformed into a major platform for the delivery of multimedia supporting different types of interactions among users such as discussions, debates, educational tips, how-to's etc.

YouTube is one of the most popular and widely used video sharing websites which allows users to publicize and share their independently generated content over the internet. Research shows that YouTube has become a convenient platform for many users to share offensive and malicious information and promote their ideologies. This led YouTube to become a repository of large amounts of malicious and offensive videos. For example, harassment and insulting videos [9], video spam [2], pornographic content [2] [12], hate and extremism promoting videos [6]. Despite several community guidelines[1] and administrative efforts made by YouTube, an old troubling problem with a new face, i. e. cyberbullying has found its way into the web.

Cyberbullying is defined as an aggressive, intentional act carried out by a group or individual, using electronic forms of contact, repeatedly and over time, against a victim who cannot easily defend himself or herself [4]. Initially, though cyberbullying may not seen to cause any physical damage, but there are some potentially disturbing examples like bullied person has gone through depression, low self-esteem, suicide ideation, and even suicide [15]. Hannah Smith, a 14-year-old, hanged herself after negative comments were posted on her Ask.fm page, a popular social network among teenagers[2]. According to Cyberbullying

---

Research Center[3], cyberbullying was a contributing factor in her death.

Detection of cyberbullying and finding preventive measures are the main areas of focus in combating cyberbullying. In the context of YouTube cyberbullying can be an unauthorized shooting or uploading negative video of a claimant on website. The aim of this paper is to counter and combat cyberbullying and misdemeanor activities on YouTube, since the instances of cyberbullying on YouTube have become an increasing concern. YouTube is a dynamic website and hence identifying cyberbullying content on

YouTube is a challenging problem. Therefore our work presented in this paper is motivated by the following facts:

a) YouTube's popularity, anonymity and low publication barriers allow users to upload cyberbullying and misdemeanor promoting content.

b) Limitations in solution capabilities being used by YouTube for cyberbullying detection.

c) Developing a systematic framework for automatic identification and to combat and counter cyberbullying videos on YouTube.

The research aim of the work presented in this paper is following:

a) The identification and characterization of such videos and users, promoting cyberbullying (Focus of this paper) on YouTube.

b) To investigate the effectiveness a Shark Search algorithm based approach for detecting YouTube videos and users promoting cyberbullying. Our aim is to examine the significance of the proposed approach.

c) To investigate the effectiveness of several contextual features in cyberbullying detection.

d) To discover users and/or communities playing central role in spreading cyberbullying and online harassment.

II. RELATED WORK & RESEARCH CONTRIBUTIONS

We conduct a literature survey in the area of cyberbullying, offense, online harassment and abusive content detection on popular social networking websites. However, based on our review of existing literature, we conclude that most of the researches for cyberbullying detection are performed in the field of mining media like, images & video frames and user generated content like, comments & messages.

For identifying privacy invasion and misdemeanor on YouTube, Nisha Aggarwal et. al. [1] proposed one class classifier approach and performed a characterization study on several sub problems: detection of vulgar video, abuse &

violence in public places and detecting videos of ragging in school and colleges.

Vidushi Chaudhary et. al. [2] has recognized promotional videos, pornographic or dirty videos and automated scripts or botnet responses in YouTube corpus by formulating the video response spam detection problem as a one-class classification problem.

For detecting cyberbullying in MySpace corpus, Maral Dadvar et. al. [4] investigated a gender-specific text classifier approach. They have utilized content based and user based features along with Vector Machine model for training text classifier using WEKA.

Analysis of the language used for bullying has been done by April Kontostathis et. al. [7] and the research has extended by using supervised machine learning approach on labeled data, in conjunction with techniques provided by the WEKA Tool Kit to train the computer to recognize cyberbullying content.

Ying Chen et al. [8] investigated existing text mining methods for detection of offensive contents to protect adolescent's online safety, using proposed Lexical Syntactic Feature (LSF) architecture.

Dawei Yin et. al. proposed supervised learning approach for detecting harassment. They determined that identification of online harassment is feasible when Term Frequency Inverse Document Frequency (TFIDF) is supplemented with N-gram and contextual feature attributes [9].

Jun-Ming Xu et. al. introduced social media as a large-scale, near real-time, dynamic data source for the study of bullying. They formulated cyberbullying detection as Natural Language Processing (NLP) tasks [17].

In a recent study on cyberbullying detection, Homa Hosseinmardi et. al. [16] investigates approaches for automatic detection of cyberbullying over Instagram. They device Naïve Bayes and linear SVM classifiers on a sample data set from Instagram consisting of manually labeled images and their associated comments.

Lots of previous work in cyberbullying detection has mostly concentrated on the media key frame based analysis & related solutions. Christian Jansohn et. al. [11] proposed conventional key frame based methods with statistical analysis of MPEG-4 motion vectors. Whereas, Nilesh J. Uke et. al. [12] proposed an approach which consists of segmentation and classification phases for extracting the key frames in nude images, and segregation of objectionable videos, respectively. Later, the videos were marked as porn or non-porn depending upon the judgment criteria.

In context to existing work, the study presented in this paper makes the following unique contributions:

a) In comparison to previous work, the work presented in this paper is first step towards application of Shark Search algorithm based approach for detecting

---

cyberbullying content on YouTube, using video metadata and contextual features.

b) We conduct a series of experiments on real-world data fetched from YouTube to demonstrate the effectiveness of the proposed solution.

c) We perform a characterization study of the cyberbullying promoting videos based on terms present in the video title & description, YouTube category, content focus and average length of videos.

III. PROPOSED SOLUTION APPROACH

Our goal is to identify cyberbullying (intentional or un-intentional) on YouTube, one of the most popular video sharing website today. We purpose a mechanism for identifying videos and users promoting cyberbullying. This proposed system incorporates a set of video attributes, discriminatory features and classification algorithm. To achieve our goal, we collected required dataset from YouTube. We evaluate the effectiveness of proposed approach using a test dataset, which was then built from a sample of the collected data.

Our proposed framework is described in section A, whereas; section B presents implementation details.

A. Proposed System

Fig. 1 presents a general research framework for proposed approach. As shown in Fig. 1, the proposed approach is a multi-step process consisting of three phases; namely, training & testing profiles collection, dynamic model building and implementation based on Shark Search algorithm.

Phase 1: Training & Testing Profiles Collection

Phase 2: Features Extraction & Dynamic Model Building
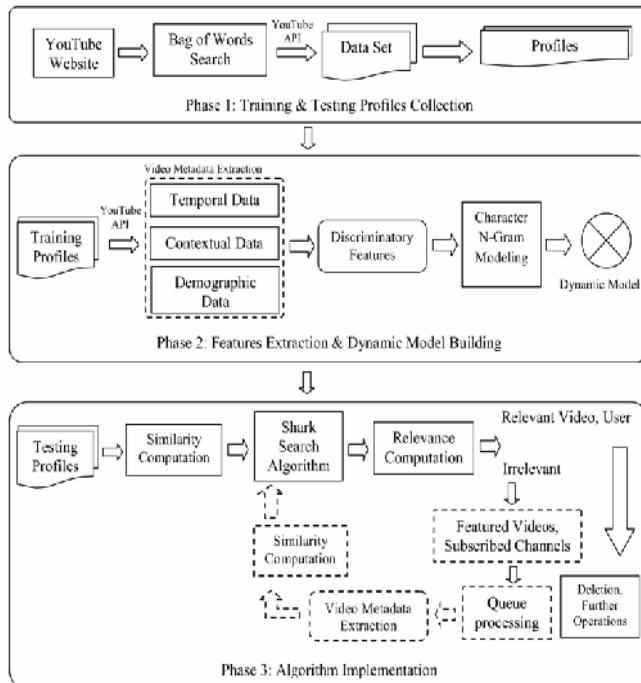
Phase 3: Algorithm Implementation

Fig. 1. General Research Framework for Proposed Solution Approach

In phase 1, we first perform a manual analysis along with visual inspection of YouTube videos and its contextual metadata. Using YouTube API[4], we build & collect our training dataset by retrieving all the available meta-data of several relevant (positive class) videos. In the training dataset, we observe several terms relevant to cyberbullying which contributes to next step of characterization and identification of discriminatory features. The retrieved meta-data of training dataset serve as a base for various discriminatory features, like, temporal and popularity based features (no. of subscribers, likes, dislikes, views and comments posted in response to the video), linguistic features (title and description of the video) and time based features (duration of video, upload time-stamp).

In phase 2, we build a dynamic model from these training profiles. For this purpose, we use character n-gram based approach, as it does not require extensive language specific pre-processing.

In phase 3, we build a system based on Shark Search algorithm which is a recursive process operates on testing dataset. It takes YouTube video as a seed and finds the textual similarity between seed video meta-data and training data. We implement a binary classifier to classify a video as relevant or irrelevant. A video is said to be relevant i.e. cyberbullying promoting video if its computation score is above the predicted threshold. Irrespective of the relevance, we further extend video frontiers like links to other YouTube videos; subscribers of the channel; featured channels or videos, suggested or related videos. We extract these frontiers by using HTML parser library[5] and YouTube API features.

B. Solution Implementation

In this section, we present the methodology and solution implementation details for the general research framework articulated in the previous section. In proposed solution we use Shark Search Algorithm (SSA). The goal of SSA is to first classify a video to be relevant (positive class) or irrelevant (negative class) and then explore the frontiers of both types of videos.

Inputs to this algorithm are seed (a video) U, threshold th for classification, n-gram value Ng for similarity computation. We compare each training profile meta-data with all n-gram values in bag-of-words collected using

---

standard dictionary[6]and compute their similarity score for each seed in testing dataset.

1) Shark Search Algorithm

We propose a Shark Search Algorithm (Algorithm 1), which is an adaptive version of the algorithm introduced in [1]. The proposed method (Algorithm 1) explores frontiers of both relevant and irrelevant videos to seed input. Steps 1 and 2 extract all contextual features for training profiles using Algorithm 2 and build a training data set. Algorithm SSA is a recursive function which takes U as a seed input. Steps 3 and 4 extract all features for seed user U and compute its similarity score with training profiles using character n-gram and probability of maximum likelihood. Steps 5 to 8 represent the classification procedure and labeling of videos as relevant or irrelevant.

Steps 10 to 14 extract frontiers of a user channel using Algorithm 3 and repeats steps 3 to 14 for each linked video.

2) Features Extraction

In Algorithm 2, we retrieve contextual metadata of a YouTube user channel and video using YouTube API. Step 1 extracts the profile summary of the user. Steps 2 to 5 extract the titles of videos uploaded, commented, shared and marked favorite. The result of this algorithm can be stored in a text file containing all video titles and user profile information.

3) Frontiers Extraction

In Algorithm 3, we extract all external links of a YouTube video to other YouTube videos. These links could be the subscribers, featured videos or channels, and related videos. YouTube API does not allow users to retrieve the information of other users which is why we use HTML parser library to fetch all frontiers.

Data: Seed Video U, Threshold th, N-gram N_g
Result: List of Relevant and Irrelevant Videos
1. for all $u\ \mathcal{E}\ U$ do
2. $D.add(ExtractFeatures(u))$
  end
  Algorithm $SSA\ (U)$
3. videofeeds $U_f \leftarrow ExtractFeatures(U)$
4. score $s \leftarrow LikelihoodProbability(D, U_f, N_g)$
5.   if $(s < th)$ then
6. $U.newclass \leftarrow$ Irrelevant
7.   else
8. $U.newclass \leftarrow$ Relevant
  end
9. Hashmap $U_{sorted}.InsertionSort(U, s)$
10. for all U_g do
11. $fr = Extract\_Frontiers(U_g)$

12.   Hashmap $U_{crawler}.add(fr)$
  end
13. for all $U_{fr}\ \mathcal{E}\ U_{crawler}$ do
14. $SSA(U_{fr})$
  end
 end
Algorithm 1. Shark Search Algorithm

Data: User Video u
Result: Video Information
   Algorithm $ExtractFeatures(U)$
1. $u_{Profile} \leftarrow$ u.getSummary()
2. $u_{Uploads} \leftarrow$ u.getUploadedVideo()
3. $u_{Commented} \leftarrow$ u.getCommentedVideo()
4. $u_{Shared} \leftarrow$ u.getSharedVideo()
5. $u_{favorited} \leftarrow$ u.getFavoritedVideo()

Algorithm 2. Features Extraction Algorithm

 Data: User Video u
 Result: Frontiers of a Video
   Algorithm Extract_Frontiers(U)
1. $u_{subs} \leftarrow$ u.getSubscribers()
2. $u_{fc} \leftarrow$ u.getFeaturedChannels()
3. $u_{rv} \leftarrow$ u.getRelatedVideos()

Algorithm 3. Frontiers Extraction Algorithm

IV. Analysis & Performance Evaluation

In this section we present the characterization and empirical analysis of cyberbullying videos. We describe the experiments and analysis set up, calculate performance and the effectiveness of our proposed solution approach.

A. Experimental Dataset

1) Training Dataset

Our proposed solution needs to classify a given video is relevant or not with respect to cyberbullying. The SSA requires sample documents or training dataset to learn the specific characteristics and properties of videos, users promoting cyberbullying. We perform a survey and manual analysis on YouTube and query for several cyberbullying and harassment keywords. Table I shows 41 keywords from a list used for building training profiles. These keywords help to collect 997 videos using YouTube API. Initially we collect 151 relevant videos, and later we extract 846 videos. Hence in total we collect a testing data set of 997 videos for cyberbullying detection. We make sure that there is no redundancy in the training dataset. We identify discriminatory features from videos of training dataset. We believe that the discriminatory features of such videos reacts

---

[6] http://www.noswearing.com/dictionary

user interests and can be used for building a predictive model.

2) Test Dataset

We create a test dataset of 997 videos by extracting the positive as well as negative class videos on YouTube. Table II shows the size of training and test dataset we collected for cyberbullying detection.

Our training dataset includes positive class videos and the test dataset includes both positive and negative class videos. Therefore, the size of training dataset is smaller than the test dataset. We annotate the dataset and label each video as relevant or irrelevant

TABLE I: A SAMPLE LIST OF KEYWORDS PRESENT IN CYBERBULLYING AND MISDEMEANOR PROMOTING VIDEOS

Terms	People Type	Examples of Video Title
hot, private, removing, MMS, sexy, kiss, nipple, breast, ass, removing, porn, boob, hottest, naked, sex, f**k, smooching, secret, sexy, seduce, lovers, scandal, kissing, sexually, harassed	girls, girl, boy, gay, student, boyfriend, female, girlfriend, guys, lover, classmate, men, ladies, aunty, people, student, couple	CCTV footage Girl sexually harassed in metro MMS of girl in car MMS Kand in School
Fights, fighting, fight, brutally, violence, killed, beats, domestic, beaten, mess, scolding, beaten	Student, kids boy, girl, girls gay, dudes, boy, student, teacher, friends, police, aunty, man, women, people, women, girls	Teacher Slaps Student In Class BRUTAL BEATING High School Boy VICIOUSLY BEATS A Girl In The Hallway
Ragging, ragged, horrible, shocking	Girl, seniors, student, juniors, students, junior, senior, fresher	Bully Ragging An Innocent Boy.wmv SHOCKING VIDEO OF RAGGING EMERGES

TABLE II: SIZE OF THE EXPERIMENTAL DATASET

Training Dataset	Testing Dataset
151	997

TABLE III: CONFUSION MATRIX

		Predicted	
		Relevant	Irrelevant
Actual	Relevant	187	78
	Irrelevant	85	647

TABLE IV: PERFORMANCE RESULTS

FPR	TNR	Precision	Recall	F-Score	Accuracy
0.1161	0.8838	0.6875	0.7056	0.6965	0.8365

B. Evaluation Metric

To evaluate the effectiveness of the proposed solution approach, we have used a standard confusion matrix with each column of the matrix representing the predicted class instances while each row of the matrix representing the actual class instances. Each position in the confusion matrix represents the number of elements belonging to that particular class.

Table III shows the confusion matrix for proposed solution approach. We execute SSA classifier for test dataset of 997 videos and it classifies 272 (187+85) videos as relevant and 725 (78+647) videos as irrelevant. Table III reveals that 85 and 78 videos are misclassified as relevant and irrelevant respectively. There are several reasons of this misclassification. Few of them are listed below:

a) Presence of noisy data such as, misleading information, misspelled words and lack of information. For example, "Brutal pelea campal todos contra todos Brutal pitched battle all against all" video is misclassified as irrelevant because of noisy data. The video "Sexual Harassment" is misclassified as relevant because of lack of information

b) Presence of commercial, news and advertising videos on YouTube. For example, a video titled "Workplace Issue Sexual Harassment" is posted on YouTube for the public awareness but due to the presence of terms sexual and harassment in title, this video is misclassified as a positive class video.

We evaluate the performance of our proposed solution approach in terms of False Positive Rate (FPR), True Negative Rate (TNR), Precision, Recall, F-score and Accuracy. Table IV shows the performance evaluation of our proposed solution approach. Table IV reveals that overall accuracy for cyberbullying detection is 83.65%.

C. Empirical Analysis

We identify all discriminatory contextual features to detect cyberbullying promoting videos, users on YouTube. We characterize each video by its meta-data. This set of contextual features is divided into 4 categories: linguistic, YouTube basic, temporal and popularity based, and time based features.

a) *Linguistic features:* We hypothesize that percentage of cyberbullying terms in title (PCTT) and description (PCTD) is an indicator to recognize relevant videos. Our hypothesis is based on the observation that more than 72% positive class videos contain some cyberbullying and misdemeanor terms in title while more than 69% negative class videos contain negligible amount of relevant terms in title (Fig. 2) and around 76% relevant videos contain some cyberbullying terms present in description while around 52% negative class videos does not contain any relevant terms in description of that video (Fig. 3) which shows the discriminatory behaviour of the feature. We use a standard dictionary of cyberbullying & negative words to match predefined terms in title and description of video.

b) *YouTube Basic Features*: Category of the video (CV) is the feature which shows the type of the video (education, entertainment, news etc.) to which it belongs. A visual inspection of multiple cyberbullying videos across their category shows the discriminatory behaviour of the feature as out of total 32 YouTube video categories, 26% cyberbullying videos fall under the category entertainment and 35% cyberbullying videos are of category people & blogs (Fig. 4).
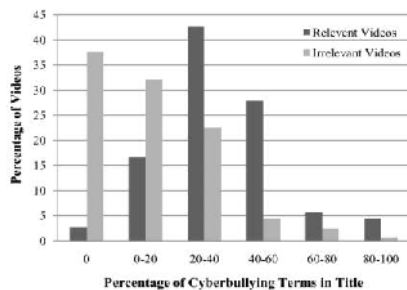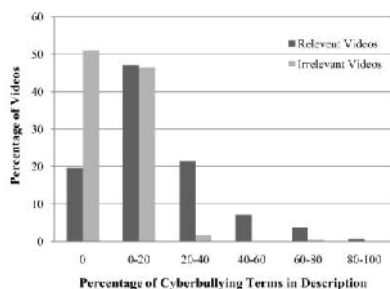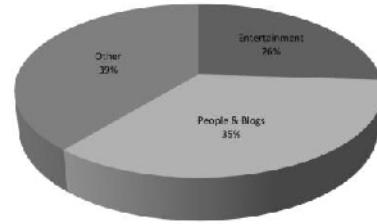

Fig. 4. CV

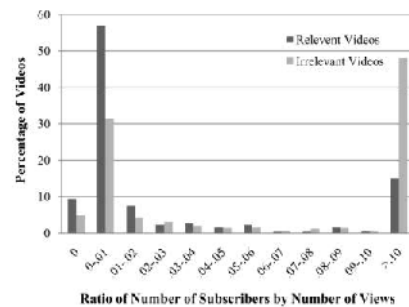Fig. 5. RSBV
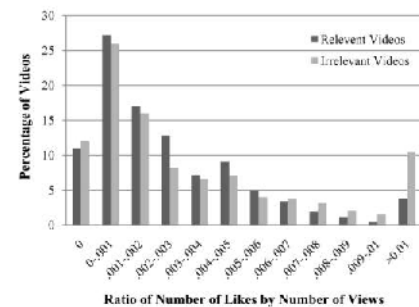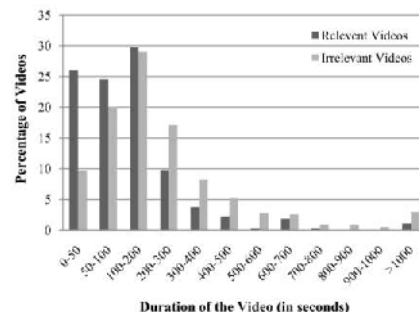

Fig. 6. RLBV

Fig. 7. DYTV

Fig. 2. PCTT

Fig. 3. PCTD

c) Temporal and Popularity Based Features: Change in features value with time shows the popularity of the videos on YouTube. Features like number of subscribers, likes, dislikes and views comes under the category Temporal and Popularity. We fetch the number of subscribers, likes and views of each video response present in our training dataset and compute the ratio of number of subscribers by number of views (RSBV) and number of likes by number of views (RLBV). These values can be a good indicator to detect cyberbullying videos. We hypothesize that low value of RSBV and RLBV signals pornographic behaviour. We confirm the effectiveness of this phenomenon in the evaluation dataset wherein the RSBV and RLBV exhibit a low value as around 70% positive class videos have RSBV value less than 0.01 while around 65% negative class videos have RSBV value greater than 0.01 (Fig. 5) and around 40% positive class videos have RLBV value less than 0.001 while 62% negative class videos have RLBV value greater than 0.001 (Fig. 6).

d) Time Based Feature: We observe the pattern of duration of multiple YouTube videos (DYTV). It clearly shows that duration of the video is a good indicator for relevant video detection as around 26% cyberbullying videos have duration less than 50 seconds and more than 51% videos have duration less than 100 seconds while around 71% irrelevant videos have duration greater than 100 seconds (Fig. 7).

CONCLUSION

Cyberbullying is a serious problem in online social networks and becoming a major threat to teenagers and adolescents. In this paper, we presented Shark Search algorithm based classification approach for automatic identification of users, videos promoting cyberbullying on YouTube. Our findings and performance evaluation result reveals that, the proposed solution approach correctly able to identify cyberbullying promoters with 83.65% accuracy.

Our results showed that, incorporation of various discriminatory features like linguistic features, popularity based features, temporal features, time based features and other reliable contextual meta-data significantly improves cyberbullying and misdemeanor detection accuracy.

Future Work

In future stages this work could be extended by considering performance of our proposed system on larger and more diverse training & testing dataset. One future direction along the proposed line of research could be to find the performance of text classifier considering language independence. Additionally, further future work requires an investigation of techniques for cyberbullying videos that do not contain any relevant meta-data and on which text classification cannot be applied.

REFERENCES

[1]. Nisha Aggarwal, Swati Agrawal, Ashish Sureka, "Mining YouTube Metadata for Detecting Privacy Invading Harassment and Misdemeanor Videos," Twelfth Annual International Conference on Privacy, Security and Trust (PST), IEEE, pp. 84 – 93, 2014.

[2]. Vidushi Chaudhary, Ashish Sureka, "Contextual Feature Based One-Class Classifier Approach for Detecting Video Response Spam on YouTube," Eleventh Annual International Conference on Privacy, Security and Trust (PST), IEEE, pp. 195 – 204, 2013.

[3]. Swati Agarwal, Ashish Sureka, "A Focused Crawler for Mining Hate and Extremism Promoting Users, Videos and Communities on YouTube," 25th ACM conference on Hypertext and social media, pp. 294-296, 2014.

[4]. Maral Dadvar, Franciska de Jong, "Cyberbullying Detection; A Step Toward a Safer Internet Yard," 21st international conference companion on World Wide Web, ACM, pp. 121-126, 2012.

[5]. Maral Dadvar, Dolf Trieschnigg, Roeland Ordelman, Franciska de Jong, "Improving Cyberbullying Detection with User Context," 35th European Conference on IR Research, Springer, pp. 693-696, 2013.

[6]. Ashish Sureka, Ponnurangam Kumaraguru, Atul Goyal, Sidharth Chhabra, "Mining YouTube to Discover Extremist Videos, Users and Hidden Communities," 6th Asia Information Retrieval Societies Conference, Springer, pp. 13-24, 2010.

[7]. April Kontostathis, Kelly Reynolds, Andy Garron, "Detecting Cyberbullying: Query Terms and Techniques," 5th Annual ACM Web Science Conference, pp. 195-204, 2013.

[8]. Ying Chen, Sencun Zhu, Yilu Zhou, Heng Xu, "Detecting Offensive Language in Social Media to Protect Adolescent Online Safety," ACM, 2012.

[9]. Zhenzhen Xue, Dawei Yin, Liangjie Hong, Brian D. Davison, April Kontostathis, Lynne Edwards, "Detection of Harassment on Web 2.0," CAW2.0, 2009.

[10]. Paridhi Singhal, Ashish Bansal "Improved Textual Cyberbullying Detection Using Data Mining", International Journal of Information and Computation Technology, pp.569-576, 2013.

[11]. Christian Jansohn, Adrian Ulges, Thomas M. Breuel, "Detecting Pornographic Video Content by Combining Image Features with Motion Information," ACM, pp. 601-604, 2009.

[12]. Nilesh J.Uke, Dr. Ravindra C. Thool, "Detecting Pornography on Web to Prevent Child Abuse – A Computer Vision Approach," International Journal of Scientific & Engineering Research, pp. 1-3, 2012.

[13]. Sara Owsley Sood, Elizabeth F. Churchill, Judd Antin, "Automatic Identification of Personal Insults on Social News Sites," Journal of the American Society for Information Science and Technology, ACM, pp. 270-285, 2012.

[14]. Laura P. Del Bosque, Sara E. Garza, "Aggressive text detection for cyberbullying," 13th Mexican International Conference on Artificial Intelligence, Springer, pp. 221-232, 2014.

[15]. Hinduja, S., and Patchin J. W., "Cyberbullying research summary, cyberbullying and suicide," 2010.

[16]. Homa Hosseinmardi, Sabrina Arredondo Mattson, Rahat Ibn Rafiq, Richard Han, Qin Lv, Shivakant Mishra, "Detection of Cyberbullying Incidents on the Instagram Social Network," Association for the Advancement of Artificial Intelligence, ARXIV, 2015.

[17]. Jun-Ming Xu, Kwang-Sung Jun, Xiaojin Zhu, Amy Bellmore, "Learning from bullying traces in social media," NAACL HLT '12 Proceedings of the 2012 Conference of the North American Chapter of the Association for Computational Linguistics: Human Language Technologies, ACM, pp. 656-666, 2012.

● ● ●